The Price of Violence: The Impact of Social Unrest on Real Estate in Santiago, Chile.

Ignacio Aravena-Gonzalez*

February 2, 2026

Click here for the latest version

Abstract

I estimate the causal effect of urban violence hotspots on real estate outcomes using the October 2019 social unrest in Santiago, Chile. Combining georeferenced incident hotspots from the national prosecutor's office with the universe of property transactions, I implement difference-in-differences and event-study designs with block, month, and municipality-by-year fixed effects. Residential prices in blocks with moderate to high violence exposure experience price declines of about 5–6% relative to controls, while low-exposure areas show no detectable effect. These discounts persist and grow over five years and are smallest during the metro-closure phase, when an accessibility mechanism would predict the largest impacts; furthermore, they increase after service resumed and COVID restrictions ended. To separate violence from accessibility disruptions, I classify blocks into mutually exclusive channels (Violence Only, Metro Only, Both, Control) and estimate a triple-difference decomposition. Both approaches indicate that residential price effects are driven by violence exposure rather than proximity to closed stations. Residential transaction volumes do not differentially decline, suggesting adjustment occurs primarily through prices. In contrast, commercial price effects are not significant, but violence exposure substantially reduces the probability of any commercial transaction, consistent with market thinning and potential selection among observed sales. Effects are concentrated in medium- and high-socioeconomic-status neighborhoods and in central municipalities, consistent with greater sensitivity to perceived safety risks among higher-income buyers.

Keywords: Urban violence, real estate, disamenities.
JEL Codes: R21, R23, D12, O18.

*London School of Economics and Political Science. i.a.aravena-gonzalez@lse.ac.uk

1 Introduction

Episodes of civil unrest have become a recurring feature of urban life (Haig et al., 2020). Yet we know far less about their medium- and long-run effects on real estate markets than we do about routine crime or conventional urban disamenities. This gap matters because property prices embed forward-looking beliefs about neighborhood quality and future urban trajectories. If unrest leaves persistent discounts, it points to durable changes in perceived neighborhood desirability rather than short-lived disruption.

This paper estimates the causal effect of the October 2019 social unrest in Santiago, Chile on residential and commercial real estate outcomes. What began on October 18 as protests against a marginal subway-fare increase escalated into the largest episode of unrest in Chile's recent history, with arson, looting, and damage concentrated along commercial corridors, historic landmarks, and around metro infrastructure. I combine geocoded clusters of violent events recorded over more than five months by the national prosecutor's office (*Fiscalía Nacional*) with the universe of property transactions to measure exposure at the census-block level.

The main finding is a large and persistent residential price discount in blocks with moderate to high violence exposure. Relative to non-exposed blocks, residential prices fall by about 5–6%, and the discount persists more than five years after the onset of unrest. Rental markets display a similar pattern, consistent with a sustained deterioration in perceived neighborhood desirability. In contrast, commercial price estimates are imprecise, but commercial markets contract sharply along the extensive margin, with a persistent decline in the probability of any transaction. This pattern suggests market thinning and selection into trading rather than clean price adjustment.

Identification is challenging because violence was not randomly assigned. Unrest clustered near metro stations and economically active locations that differ systematically from other areas of the city. I address this concern by exploiting the fact that metro stations experienced heterogeneous damage and closures for up to a year, creating variation in transit disruptions that do not perfectly overlap with violence hotspots. I classify blocks into mutually exclusive exposure channels—*Violence Only*, *Metro Closure Only*, *Both*, and *Control*—and estimate difference-in-differences event-study models with block, year-month and municipality-by-year fixed effects that absorb granular time-varying local shocks. I complement this approach with triple-difference specifications that decompose violence intensity, proximity to closed stations, and their interaction.

Two dynamic patterns further inform interpretation. First, residential effects are smallest during the metro-closure phase and largest once the metro service wass restored and COVID restrictions end. This timing is difficult to reconcile with a pure accessibility mechanism. Second, blocks in the *Violence Only* channel experience persistent price declines, whereas blocks in the *Metro Only* channel do not show robust negative effects. Together, these results point away from transit access losses as the main driver and lean toward a violence-related channel consistent with reputational scarring.

The key conceptual distinction is between temporary disruption and durable damages. In standard hedonic models, violence is a local disamenity and should reduce neighborhood desirability and prices (Thaler, 1978; Gibbons, 2004). Whether these effects persist, however, depends on beliefs. If the episode is perceived as transitory, capitalization should fade; if it changes perceived neighborhood safety, identity, or the level of amenities, it can generate stigma with long-lived (or even growing) effects (Gourley, 2019). More broadly, studies find that higher crime exposure is associated with lower property values, with magnitudes varying by crime type and spatial scale (Gibbons, 2004; Braakmann, 2017; Ceccato and Wilhelmsson, 2011, 2020; Lens and Meltzer, 2016). Evidence from point-event settings shows that housing market responses can be highly localized (Klimova and Lee, 2014; Linden and Rockoff, 2008), and crimes signaling disorder or personal risk generate larger responses than property crime (Gibbons, 2004; Linden and Rockoff, 2008).

This paper contributes to three strands of literature. First, it provides causal evidence on unrest and real estate from a major Latin American city using granular administrative microdata and validated geocoding of exposure. While prior work has examined riots in the United States (Collins and Margo, 207) and conflict in Europe (Besley and Mueller, 2012; Kourtis et al., 2020), many studies rely on aggregated data—such as neighborhood-level rents —which may obscure heterogeneity and limit causal inference. The Chilean setting offers the universe of property transactions matched to validated, georeferenced incident data, enabling precise measurement of both exposure and outcomes. My estimates of 5–6% price declines are somewhat smaller than those found in less granular settings, consistent with attenuation from measurement error in coarser designs (Collins and Margo, 207; Kourtis et al., 2020). A smaller literature examines discrete shocks to violence and unrest. Besley and Mueller (2012) estimate a "peace dividend" in Northern Ireland; Collins and Margo (207) document long-lasting effects of 1960s riots in Cleveland with estimates ranging from 10–20% depending on specification. Related work shows that perceived risk from salient events can affect markets through reputation even without physical destruction (Abadie and Dermisi, 2008; Gourley, 2019). Kourtis et al. (2020) find riot-related price effects in London of 5–15%, though their estimates face challenges separating violence from concurrent neighborhood changes.

Second, the paper contributes methodologically by showing how channel classification combined with a triple-difference decomposition can help separate violence from correlated accessibility shocks in settings where multiple channels move together. This approach builds on recent advances in difference-in-differences with staggered or heterogeneous treatment (de Chaisemartin and D'Haultfœuille, 2020; Callaway and Sant'Anna, 2021) and extends mechanism-separation strategies developed in the crime capitalization literature (Linden and Rockoff, 2008; Klimova and Lee, 2014).

Third, the findings speak to broader questions of persistent urban change after acute shocks (Davis and Weinstein, 2002; Collins and Margo, 207). The persistence of effects five years after the 2019 events—their growth over time rather than decay, and their concentration in higher-status neighborhoods—suggests that violence can durably alter the urban landscape through reputational channels. This has implications for post-crisis urban policy and the design of interventions to support affected neighborhoods. The dynamic pattern and concentration in higher-income areas connect to work on information, stigma, and perceived risk in shaping neighborhood trajectories (Gourley, 2019; Abadie and Dermisi, 2008).

The remainder of the paper proceeds as follows. Section 2 describes the October 2019 unrest and institutional setting. Section 3 presents the data and exposure measures. Section 4 outlines the empirical strategy. Section 5 reports the main results. Section 6 examines mechanisms and heterogeneity. Section 7 presents robustness checks. Section 8 concludes.

2 The October 2019 Social Unrest

On October 18, 2019, protests against a CLP 30 increase[1] in Santiago's metro fare escalated into the largest episode of civil unrest in Chile's recent democratic history (Gonzalez and Morán, 2020; Cox et al., 2024). What began as student-led fare evasion quickly expanded into broader demonstrations over inequality, pensions, healthcare, and the cost of living, among other grievances (Avendaño, 2019; Sasse, 2019). Within days, protests spread across Santiago and other major cities, with large marches centered on Plaza Italia (renamed "Plaza de la Dignidad" by protesters), which became the symbolic heart of the movement (Gonzalez and Morán, 2020).

The unrest initiated a sequence of overlapping riots and demonstrations with potential implications for Santiago's real estate markets. Figure 1 documents the evolution of protest activity using event data from the Conflict and Social Cohesion Observatory (COES) (COES, 2020). Protest and public-disorder events rose sharply immediately after October 18, 2019 and remained elevated through early 2020, with substantially higher intensity in the Metropolitan Region than in the rest of the country. COES captures protest activity and disorder events recorded in media and administrative sources. The empirical analysis below measures violence exposure using geocoded criminal incidents from prosecutorial records.

The protests were accompanied by substantial violence and property damage. The

[1]CLP 30 is roughly USD 0.033 and GBP 0.025. The increase was lower than 5%.

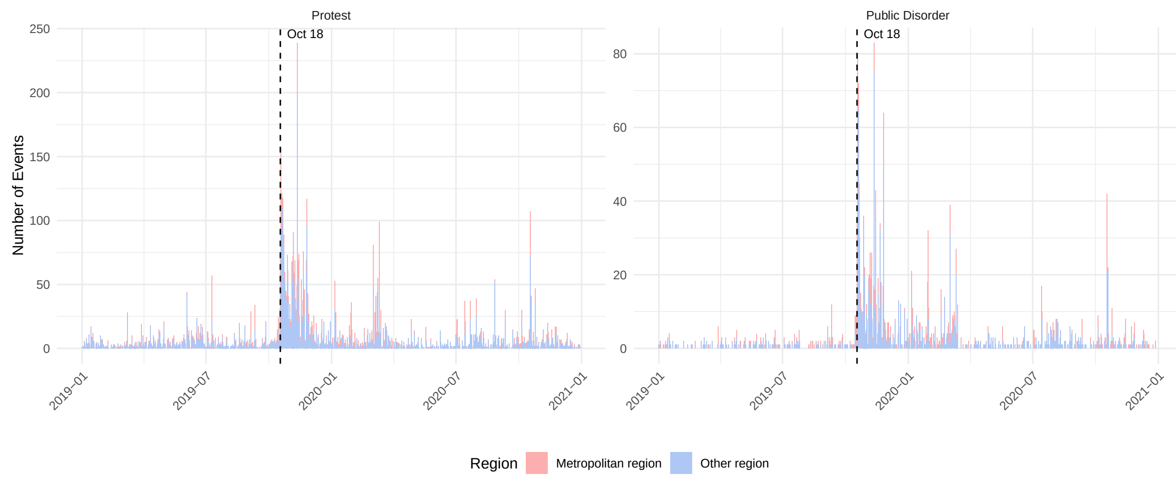

Figure 1: Protest Intensity Over Time. Weekly counts of protest events (left panel) and public-disorder events (right panel) from the COES database (COES, 2020). The vertical dashed line marks October 18, 2019. The Metropolitan Region experienced higher event counts than other regions.

Chilean Public Prosecutor's Office released an official statistical report in October 2025 consolidating all criminal cases linked to the unrest filed between October 18, 2019 and March 31, 2020 (Fiscalia Nacional, 2025). This report, which is the primary source for characterizing violence exposure in the present study, documents 32,901 cases corresponding to 35,146 criminal incidents. Incidents include institutional violence, property crimes and looting, public-disorder offenses, violence against state agents, and arson.

Santiago's metro system was particularly affected. According to Metro de Santiago, 118 of 136 stations suffered some degree of damage and 25 stations experienced severe fire damage, with reconstruction taking months for the most affected locations. Metro progressively restored service across the network, reaching full operational coverage by late September 2020 (Metro de Santiago, 2020). Given the metro system's role as a core determinant of commuting accessibility and a key amenity capitalized into housing values (Agostini and Palmucci, 2008), these closures represent a salient accessibility shock. At the same time, protest activity and damage concentrated around metro infrastructure, generating the spatial overlap between violence exposure and transit disruptions that motivates the channel-separation strategy developed in Section 4. The government declared a state of emergency and imposed curfews, the first since the return to democracy in 1990 (Gonzalez and Morán, 2020). The unrest also triggered a political process culminating in a national plebiscite on whether to draft a new constitution.[2]

The empirical analysis exploits this sequence to define periods with distinct combinations of shocks, including unrest-related violence, metro disruptions, and COVID-era restrictions. In particular, I distinguish a post-normalization period in which the metro service is fully restored and pandemic-related restrictions are no longer binding, allowing a cleaner assessment of persistent effects associated with earlier violence exposure.

Violence during the unrest was not uniformly distributed across Santiago. Figure 2 characterizes the spatial pattern using geocoded incidents from the Public Prosecutor's Office (Fiscalia Nacional, 2025). The left panel shows incident locations by type, including public disorder, arson, and looting. Violence concentrated along major transit corridors and around metro stations, with high intensity near Plaza Italia and extending along key axes and multiple metro lines. The center panel overlays violence buffers on neighborhood socioeconomic status, highlighting that exposure spans multiple income levels, a feature relevant for the heterogeneous effects explored in Section 6. The right panel displays the violence intensity index used in the empirical analysis, taking values $\{0, 1, 2, 3\}$ to reflect increasing exposure. The spatial coincidence between violence exposure and metro disruptions motivates the channel-separation strategy developed in Section 4.

3 Data

3.1 Data Sources

The analysis combines six data sources.

First, I use administrative records of residential and commercial property transactions in the Santiago Metropolitan Region from January 2016 through December 2024 from the *Servicio de Impuestos Internos (SII)*, Chile's tax authority. The transaction microdata are

[2] The plebiscite passed with 78% approval; the subsequent draft was rejected by voters in September 2022.

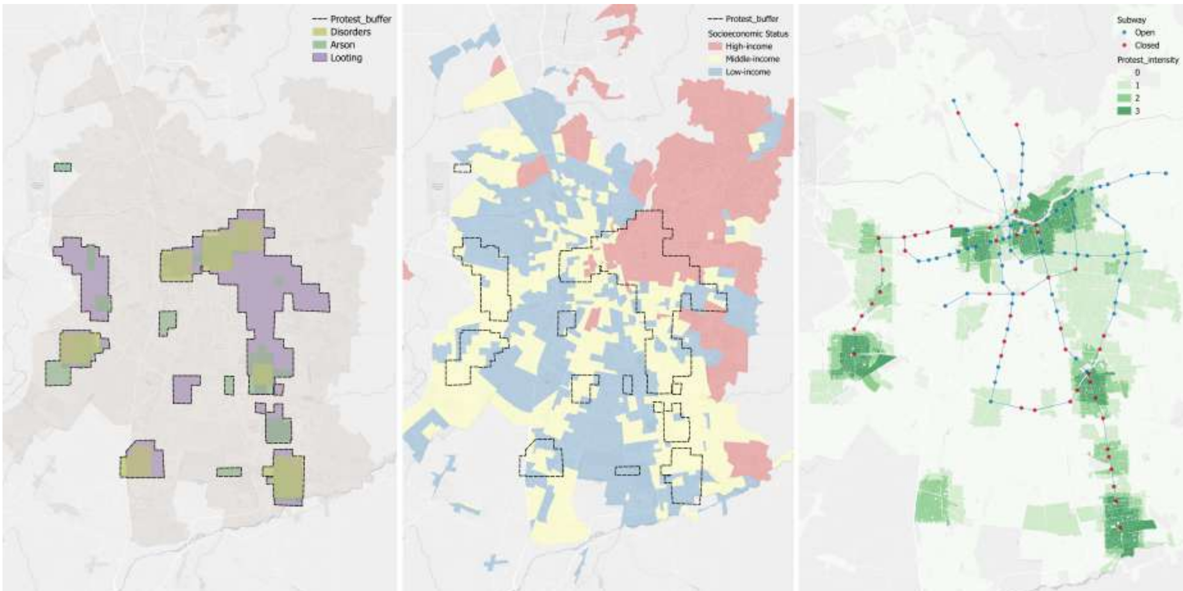

Figure 2: Spatial Distribution of Violence in Santiago. The left panel shows the location of geocoded criminal incidents during October 2019–March 2020 by type (Fiscalia Nacional, 2025). The center panel overlays neighborhood socioeconomic status by census block with violence buffers. The right panel shows the violence intensity index (0–3) overlaid with the metro network; points indicate stations that experienced closures due to damage.

assembled from multiple SII registers and harmonized into a single dataset. Each record reports the transaction price (in UF), construction area and lot size when available, year built, property type, and geographic location at the census-block (*manzana*) level. I restrict the residential sample to transactions with non-missing price and key characteristics and exclude extreme observations. The final residential sample contains 467,034 transactions across 44,699 blocks. The commercial sample contains 22,417 transactions.

Second, I complement transactions with apartment rental listings scraped from online portals. The listings dataset reports asking rents and unit attributes together with geographic coordinates. I geocode listings and assign each observation to a census block.

Third, I use georeferenced incident information from the National Public Prosecutor's Office (Fiscalia Nacional, 2025), which consolidated criminal cases linked to the unrest filed between October 18, 2019 and March 31, 2020. The Prosecutor's Office provides statistically significant spatial clusters (*hotspots*) for each incident category. I intersect these hotspot polygons with census-block polygons and assign exposure at the block level. I construct a block-level violence exposure index for October 2019–March 2020. For each block, I define three indicators for intersection with a hotspot of public disorder, arson, and looting, and sum them to obtain $V_b \in \{0, 1, 2, 3\}$. The index captures exposure to multiple incident types across categories rather than event counts.

Fourth, I use operational records from Metro de Santiago identifying stations damaged during the unrest. I compute the distance from each block centroid to the nearest closed station and define baseline metro exposure using a 500-meter threshold[3]. I measure potential accessibility disruption using distance to metro stations that were closed due to unrest-related damage, defining $M_b = 1$ if a block lies within 500 meters of any closed station. Fifth, I supplement the analysis with police crime statistics from Carabineros de Chile's *Plan Cuadrante*. This source provides annual crime counts by type at the police-quadrant level for 2018 and 2023.

Sixth, I incorporate pre-treatment Census information from 2017 on population and density at the block level and the ISMT socioeconomic index from the *Observatorio de Ciudades UC*, measured at the census-tract level (Araya, 2023).

In addition to the transaction-level dataset, I construct panels at the census-block by quarter level for residential transactions, commercial transactions, and rental listings. For each block-quarter, I compute the number of transactions as a measure of market activity and summary price measures such as mean or median log prices and mean log prices per square meter using the cleaned samples. This panel structure is used to estimate effects on transaction volumes.

3.2 Summary Statistics

Table 1 reports pre-period summary statistics by violence exposure intensity. High-intensity areas with $V = 3$ are more central, averaging 696 meters from the nearest metro station. They also have a much higher baseline commercial presence, with 13.83 commercial proper-

[3] Robustness checks consider alternative thresholds.

ties per block compared with 1.32 in control areas, and a higher socioeconomic status index, with 1.92 compared with 1.57. Residential prices follow the same gradient, increasing from 44.6 UF/m^2 in control areas to 58.4 UF/m^2 in high-intensity areas. These level differences reflect the non-random geography of unrest, which concentrated around central transit and commercial corridors.[4]

These level differences reflect the non-random geography of the unrest. Exposure is strongly linked to transit nodes, centrality, and commercially active corridors, and it also appears around secondary municipal hubs. This pattern is not captured by socioeconomic status alone. Identification in the difference-in-differences analysis therefore relies on differential changes over time, conditional on block and flexible location-time controls, rather than on balance in pre-period levels.

Figure 3 provides descriptive evidence on price dynamics. It plots hedonic price indices—residuals from a regression of log price on property characteristics, normalized to 100 in October 2017—by violence intensity. The series move similarly prior to October 2019; however, higher-intensity areas display larger and persistent declines after the shock, following a non-linear pattern in which $V = 2$ and $V = 3$ separate more sharply from the control group than $V = 1$. The divergence is gradual rather than immediate, consistent with delayed capitalization rather than a short-lived disruption.

Figure 4 plots event-study estimates for selected residential covariates. Observable characteristics are broadly stable over time, with modest changes in the apartment share and limited shifts in size composition relative to the magnitude of the price effects. Figure A.2 reports analogous results for commercial transactions and listings.

[4] Identification in the difference-in-differences analysis relies on differential changes over time rather than balance in levels.

Table 1: Summary Statistics by Violence Exposure (Pre-Period)

	V=0 (Control)	V=1 (Low)	V=2 (Medium)	V=3 (High)
Panel A: Residential transactions				
Price (UF/m^2)	44.6 (26.5)	49.5 (24.9)	53.9 (27.9)	58.4 (26.9)
Construction area (m^2)	65.3 (38.8)	65.1 (30.3)	65.7 (32.7)	63.5 (30.8)
Year built	2003.1 (19.3)	2000.4 (20.0)	1998.2 (19.6)	1997.4 (24.8)
Apartment (=1)	0.64	0.68	0.67	0.80
Observations	129,161	32,261	9,709	9,308
Panel B: Commercial transactions				
Price (UF/m^2)	67.4 (41.0)	61.1 (42.4)	66.4 (35.6)	64.2 (33.2)
Construction area (m^2)	156.1 (774.1)	279.2 (1453.6)	157.5 (261.0)	164.2 (438.6)
Year built	1998.8 (26.5)	1986.9 (30.4)	1991.7 (27.0)	1987.7 (30.6)
Office (=1)	0.62	0.56	0.60	0.73
Observations	5,339	1,144	833	1,698
Panel C: Block characteristics				
Distance to metro (m)	4,194	1,609	1,764	696
Commercial stock	1.32	1.84	4.08	13.83
GSE level	1.57	1.72	1.81	1.92
Population 2017	135	145	129	147
Blocks	34,060 (76.2%)	7,031 (15.7%)	2,263 (5.1%)	1,345 (3.0%)
Panel D: Rental listings				
Rent (UF/m^2)	0.32 (0.10)	0.30 (0.09)	0.31 (0.08)	0.33 (0.09)
Rent (UF)	29.1 (15.6)	22.8 (12.3)	23.9 (9.0)	19.3 (5.6)
Size (m^2)	96.6 (50.4)	79.5 (37.8)	81.5 (36.4)	63.2 (26.7)
Bedrooms	2.36 (0.91)	2.16 (0.82)	2.14 (0.89)	1.77 (0.84)
Bathrooms	2.08 (0.85)	1.86 (0.66)	1.91 (0.70)	1.53 (0.58)
Observations	3,858	1,318	595	657

Notes: Standard deviations in parentheses (Panels A, B, and D). Pre-period: Oct 2017–Sep 2019. Violence intensity $V \in \{0, 1, 2, 3\}$ is based on whether the block polygon intersects crime hotspots for public disorder, arson, and looting during Oct 2019–Mar 2020.

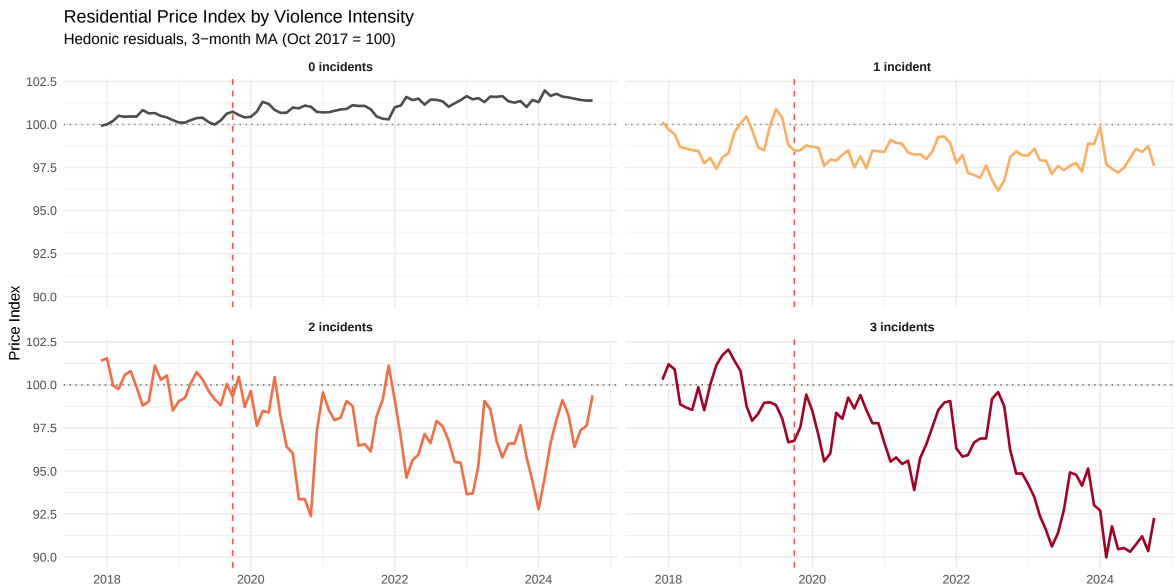

Figure 3: Residential Price Indices by Violence Intensity. Hedonic residuals normalized to 100 in October 2017 and smoothed using 3-month moving averages. The vertical dashed line marks October 2019. Figure A.1 reports analogous indices for commercial transactions and rental listings.

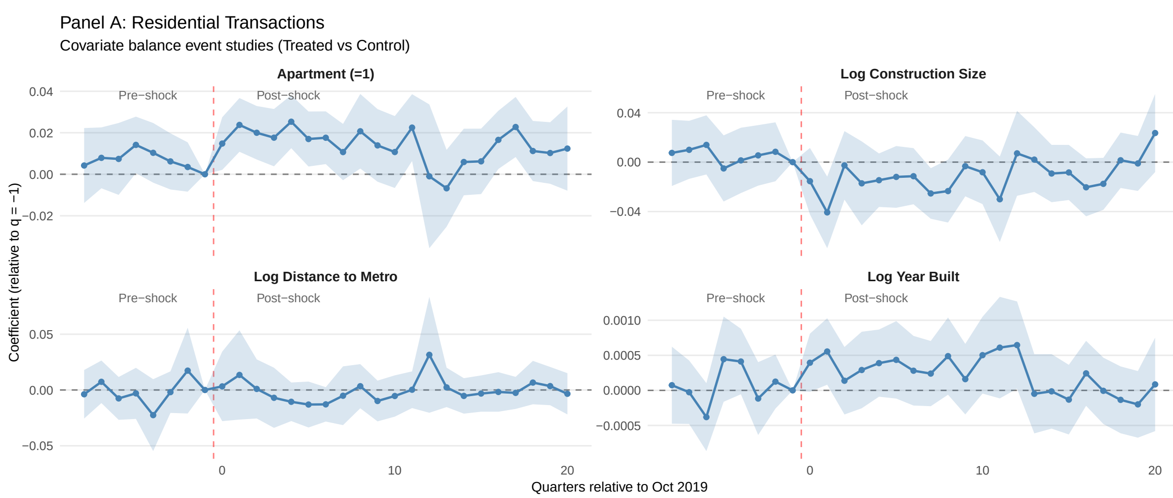

Figure 4: Covariate Balance Event Studies (Residential). Coefficients from regressions of each covariate on treated × quarter indicators with block and year-month FEs. Bands: 95% CIs, SEs clustered at block level.

4 Empirical Strategy

The October 2019 social unrest constitutes a sharp temporal shock. Identification comes from comparing prices and transaction activity before and after the shock across census blocks (*manzanas*) with different levels of exposure to unrest-related violence. The key identifying assumption is that, absent the unrest, outcomes in more- and less-exposed blocks would have evolved similarly after conditioning on a rich set of location and time controls.

A central threat to interpretation is that violence exposure is spatially correlated with centrality, commercial intensity, and metro infrastructure, which may themselves generate differential dynamics. I address this concern in two complementary ways. First, I assess pre-trends and sensitivity to flexible time controls that vary by centrality and local economic intensity (Section 7). Second, I exploit the institutional shock to the metro system, namely station damage and temporary closures, to separate violence exposure from direct accessibility disruptions.

As defined in the previous section, let $V_b \in \{0, 1, 2, 3\}$ denote violence exposure intensity for block b, constructed from prosecutorial hotspots for October 2019–March 2020. For each block, I define indicators for whether the block polygon intersects a hotspot polygon of public disorder, arson, and looting, and sum them to obtain V_b. Separately, let M_b indicate whether block b lies within 500 meters of any metro station that experienced closure due to unrest-related damage.

Combining V_b and M_b yields four mutually exclusive exposure channels: *Control* ($V_b = 0$, $M_b = 0$), *Violence Only* ($V_b \geq 1$, $M_b = 0$), *Metro Only* ($V_b = 0$, $M_b = 1$), and *Both* ($V_b \geq 1$, $M_b = 1$). The *Violence Only* channel provides the cleanest comparison for isolating violence effects net of direct accessibility shocks.

4.1 Baseline specification

Let P_{ibt} be the transaction price of property i in block b at month t. The baseline specification is:

$$\ln(P_{ibt}) = \beta\,(V_b \times \mathbb{1}\{t \geq \text{Oct 2019}\}) + X_{it}'\gamma + \alpha_b + \theta_t + \mu_{c(b),y(t)} + \varepsilon_{ibt}, \tag{1}$$

where X_{it} includes standard property characteristics (e.g., log constructed area, age controls, and property type), α_b are block fixed effects, θ_t are year-month fixed effects, and $\mu_{c(b),y(t)}$ are municipality-by-year fixed effects. Standard errors are clustered at the block level. The coefficient of interest is β, which captures the average post-shock change in log prices associated with a one-unit increase in violence exposure relative to the pre-period, conditional on the fixed effects structure.

In addition to this linear-index specification, I also estimate models that interact post indicators with exposure bins ($V_b \in \{1, 2, 3\}$, with $V_b = 0$ as the reference) to allow for non-linear dose-response patterns.

To capture dynamics and isolate a post-normalization period with minimal confounding from metro closures and COVID restrictions, I estimate event-time specifications and a phase specification that pools months into three post-shock periods: (i) *Phase 1, metro closure* (Oct 2019–Sep 2020), (ii) *Phase 2, COVID/transition* (Oct 2020–Sep 2022), and (iii) *Phase 3, post-normalization* (Oct 2022 onward). Pre-trends are assessed using event-time coefficients and joint tests of the null that all pre-shock interactions equal zero. I also implement placebo timing exercises to test whether the design mechanically produces effects at alternative dates (Section 7).

4.2 Violence versus accessibility: channel separation and triple difference

I implement two complementary designs to separate violence effects from metro-accessibility disruptions. First, I estimate specifications by exposure channel (*Violence Only*, *Metro Only*, *Both*) and allow effects to vary by phase. Second, I estimate a triple-difference specification that decomposes violence, closure proximity, and their interaction:

$$\ln(P_{ibt}) = \sum_{p} \Big[\beta_p(V_b \times \mathbb{1}\{t \in p\}) + \delta_p(M_b \times \mathbb{1}\{t \in p\}) + \kappa_p(V_b \times M_b \times \mathbb{1}\{t \in p\})\Big] \\ + X_{it}'\gamma + \alpha_b + \theta_t + \mu_{c(b),y(t)} + \varepsilon_{ibt}. \tag{2}$$

where β_p captures the marginal effect of violence intensity in areas far from closed stations ($M_b = 0$), δ_p captures the effect of closure proximity in non-violent areas ($V_b = 0$), and κ_p tests whether the violence effect differs systematically in areas also exposed to closures. A negative β_p in Phase 3, when stations have reopened and COVID restrictions have ended, is difficult to reconcile with a purely accessibility-driven explanation.

Finally, I examine heterogeneity by socioeconomic status, CBD distance, and prior crime exposure. I also analyze transaction volumes using a block-by-quarter panel constructed from the cleaned microdata. These extensions are presented in subsequent sections.

5 Main Results

5.1 Prices

Table 2 presents the main difference-in-differences estimates for residential property prices[5]. Column (1) reports a two-way fixed effects specification that treats violence exposure as a continuous index. The estimate implies that a one-unit increase in violence intensity is associated with a 2.0% price decline in the post-shock period. Given that the index ranges from 0 to 3, this corresponds to an implied discount of roughly 6% for properties in the most affected areas relative to control locations.

Column (2) adds municipality-by-year fixed effects, absorbing time-varying shocks at the municipality level that may correlate with unrest exposure. The point estimate attenuates

[5] Complete tables: Residential is in Table A.2, Commercial in Table A.3, and Rents in A.4.

to $\hat{\beta} = -0.010$, implying a more conservative average effect of roughly 3% for high-exposure areas. I treat this specification as the preferred baseline throughout the analysis.

Columns (3) and (4) show that the pooled post-shock estimate masks important dynamics. Column (3) interacts with the continuous violence index with three post-shock phases relative to the pre-period. Effects are small and statistically indistinguishable from zero during Phase 1 and Phase 2, but become sizable and significant in Phase 3. This timing provides suggestive evidence against a purely accessibility-driven explanation, which I test directly using channel separation and a triple-difference design in Section 5.2.

Column (4) corroborates this pattern using discrete exposure bins and highlights a threshold structure. Relative to pre-period control properties, Phase 3 shows sizable discounts concentrated in moderate- and high-exposure areas. Properties with $V = 2$ experience a 5.0% decline, while $V = 3$ properties show a 5.7% decline.[6] By contrast, low-exposure areas ($V = 1$) display small and statistically insignificant effects across phases. Estimates for $V = 2$ in Phase 1 are also negative, but the effects that persist and sharpen over time are concentrated in Phase 3. Overall, the nonlinear pattern is consistent with a stigmatization or disamenity mechanism in which neighborhoods must experience sufficiently salient violence to be durably marked.

Asking rents decline in violence-exposed areas, with effects that strengthen over time and concentrate in higher-intensity blocks. Regarding commercial property prices, point estimates are imprecise and not statistically distinguishable from zero across specifications. Given the smaller sample (22,417 commercial versus 467,034 residential transactions) and the scope for selection into trading,

[6] Percent changes computed as $100 \times (\exp(\hat{\beta}) - 1)$.

Table 2: Summary of Difference-in-Differences Estimates

	(1) TWFE	(2) + mun. × Year	(3) By Phase	(4) By Phase and V_b
Panel A. Residential Sales (N=467,034)				
Post × Viol. index	-0.020***	-0.010*		
Viol. index × Phase 1			-0.006	
Viol. index × Phase 2			-0.007	
Viol. index × Phase 3			-0.020***	
Phase 1 × $V = 1$				-0.014
Phase 1 × $V = 2$				-0.034**
Phase 1 × $V = 3$				-0.005
Phase 2 × $V = 1$				-0.013
Phase 2 × $V = 2$				-0.030
Phase 2 × $V = 3$				-0.010
Phase 3 × $V = 1$				-0.009
Phase 3 × $V = 2$				-0.051***
Phase 3 × $V = 3$				-0.059***
Panel B. Commercial Sales (N=22,417)				
Post × Viol. index	-0.016	0.010		
Viol. index × Phase 1			0.012	
Viol. index × Phase 2			0.025	
Viol. index × Phase 3			-0.014	
Phase 1 × $V = 1$				-0.044
Phase 1 × $V = 2$				0.053
Phase 1 × $V = 3$				0.034
Phase 2 × $V = 1$				0.075
Phase 2 × $V = 2$				0.011
Phase 2 × $V = 3$				0.075
Phase 3 × $V = 1$				0.015
Phase 3 × $V = 2$				-0.039
Phase 3 × $V = 3$				-0.048
Panel C. Apartment Listings (N=27,554)				
Post × Viol. index	-0.018***	-0.018***		
Viol. index × Phase 1			-0.015**	
Viol. index × Phase 2			-0.018***	
Viol. index × Phase 3			-0.028***	
Phase 1 × $V = 1$				-0.023
Phase 1 × $V = 2$				-0.022
Phase 1 × $V = 3$				-0.042**
Phase 2 × $V = 1$				-0.017
Phase 2 × $V = 2$				-0.015
Phase 2 × $V = 3$				-0.057***
Phase 3 × $V = 1$				-0.009
Phase 3 × $V = 2$				-0.040**
Phase 3 × $V = 3$				-0.088***
Block FE	Yes	Yes	Yes	Yes
Year-month FE	Yes	Yes	Yes	Yes
mun. × Year FE	No	Yes	Yes	Yes

Notes. Phase 1 (metro closure) is Oct 2019–Sep 2020. Phase 2 (COVID/transition) is Oct 2020–Sep 2022. Phase 3 (post-normalization) is Oct 2022 onward.
Significance. *** $p < 0.01$, ** $p < 0.05$, * $p < 0.10$.

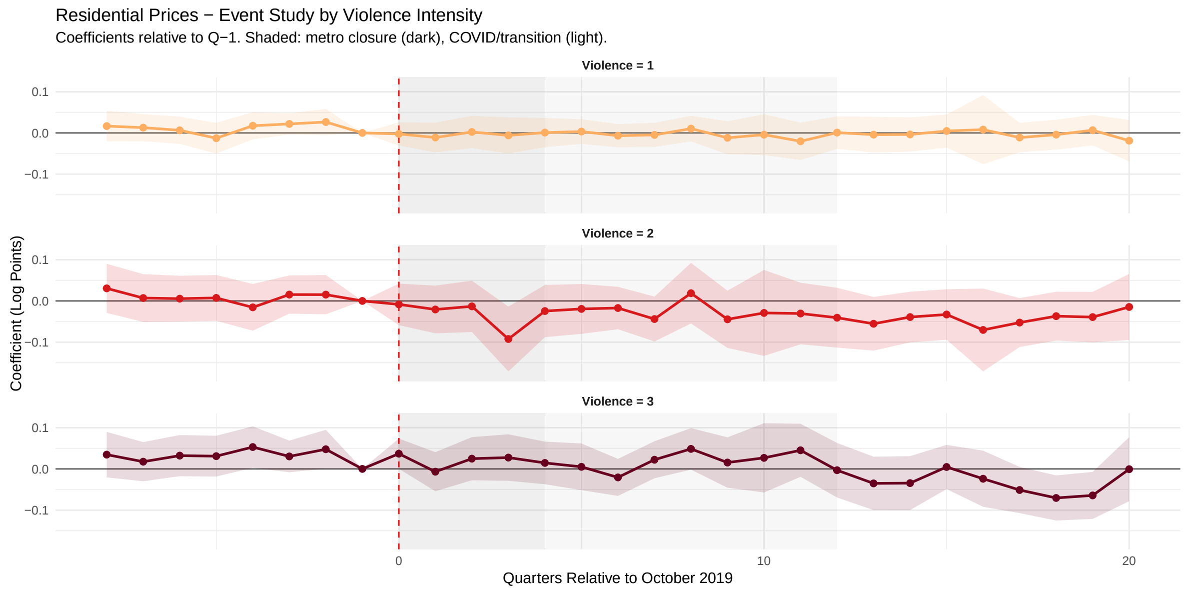

Figure 5: Residential Prices Event Study by Violence Intensity. Coefficients from a difference-in-differences event study that interacts event time (quarters relative to October 2019) with exposure groups ($V = 1, 2, 3$), using $V = 0$ blocks as the control group. Estimates are normalized to $Q{-}1$ (July–September 2019). The model includes block, year-month, and municipality-by-year fixed effects. Confidence intervals are 95% based on standard errors clustered at the block level. Shaded regions correspond to Phase 1 (metro closure) and Phase 2 (COVID/transition). The dashed line marks the shock onset ($Q0$).

Figure 5 complements Table 2 by reporting quarterly event-study estimates that trace residential price dynamics by violence intensity (Figure A.3 shows the same plots for commercial sales and apartment listing). Pre-event coefficients are close to zero and do not display systematic differential trends, supporting the identifying assumption of parallel counterfactual trends across exposure groups. The largest discounts emerge later in the sample and are concentrated in the highest exposure groups ($V = 2$ and $V = 3$), with near-zero effects for $V = 1$. The gradual divergence is consistent with delayed capitalization rather than a purely short-run disruption.

5.2 Violence versus accessibility: channel separation and triple difference

A concern is that the estimated violence effects proxy for metro-accessibility disruptions, since violence clustered around the metro during the unrest. I address this directly using a channel decomposition and a triple-difference design.

Table 3 decomposes exposure into three mutually exclusive groups, namely *Violence Only* (violence exposure but far from closed stations), *Metro Only* (near closed stations but no violence), and *Both*. The *Violence Only* channel shows a persistent Phase 3 decline of 1.8% per unit of violence intensity, and rents decline by 2.7%. In contrast, *Metro Only* estimates are small and statistically indistinguishable from zero for residential prices, which is difficult to reconcile with an accessibility-only explanation.

Table 3: Price Effects by Treatment Channel

	Residential	Commercial	Rents
Violence Only			
Phase 1	-0.0065	0.0082	-0.0154^{**}
	(0.0052)	(0.0199)	(0.0065)
Phase 2	-0.0045	0.0266	-0.0176^{***}
	(0.0064)	(0.0229)	(0.0065)
Phase 3	-0.0181^{***}	-0.0170	-0.0274^{***}
	(0.0061)	(0.0219)	(0.0079)
Metro Only			
Phase 1	-0.0053	0.2868^{**}	0.0262
	(0.0187)	(0.1447)	(0.0212)
Phase 2	0.0074	-0.1467	0.0267
	(0.0194)	(0.1521)	(0.0225)
Phase 3	0.0011	-0.1788	0.0255
	(0.0221)	(0.1427)	(0.0241)
Both			
Phase 1	-0.0028	0.0579	-0.0065
	(0.0087)	(0.0382)	(0.0110)
Phase 2	-0.0202^{**}	0.0164	-0.0165
	(0.0101)	(0.0352)	(0.0101)
Phase 3	-0.0278^{***}	-0.0005	-0.0260^{***}
	(0.0102)	(0.0375)	(0.0101)
Block FE	Yes	Yes	Yes
Year-month FE	Yes	Yes	Yes
municipality×Year FE	No	Yes	Yes
Observations	467,034	22,417	27,554

Notes: Dependent variable is log price for Residential and Commercial, and $\ln(\text{UF}/m^2)$ for Rents. Violence Only and Both coefficients are per unit of violence intensity (0–3). Metro Only is binary (near closed station, no violence). Standard errors clustered at the block level for Residential and Commercial, and at the manzana level for Rents. $^{*}p < 0.10$, $^{**}p < 0.05$, $^{***}p < 0.01$.

It is worth emphasizing that the *Both* channel mechanically selects more central locations near metro nodes. A larger coefficient for *Both* does not, by itself, establish complementarity, since it could reflect composition. The triple-difference decomposition addresses this directly.

Table 4 reports the triple-difference decomposition by phase. For residential properties, violence intensity remains negative and precisely estimated in Phase 3, while proximity to a closed station is small and statistically insignificant. Overall, the evidence supports interpreting residential discounts as operating primarily through a violence-related channel rather than temporary accessibility losses.

Table 4: Triple-Difference Decomposition by Phase

	Residential	Commercial	Rents
Violence index × Phase			
Phase 1	−0.0066	0.0063	−0.0169***
	(0.0052)	(0.0199)	(0.0064)
Phase 2	−0.0045	0.0229	−0.0188***
	(0.0064)	(0.0230)	(0.0064)
Phase 3	−0.0180***	−0.0202	−0.0287***
	(0.0061)	(0.0220)	(0.0078)
Near closed metro × Phase (binary)			
Phase 1	−0.0086	0.0882	0.0107
	(0.0191)	(0.1308)	(0.0166)
Phase 2	0.0028	−0.2351*	0.0238
	(0.0180)	(0.1220)	(0.0193)
Phase 3	0.0025	−0.2257*	0.0132
	(0.0208)	(0.1225)	(0.0169)
Violence × Near metro × Phase			
Phase 1	0.0074	0.0171	0.0145
	(0.0098)	(0.0634)	(0.0111)
Phase 2	−0.0170	0.0707	0.0014
	(0.0119)	(0.0559)	(0.0118)
Phase 3	−0.0107	0.0933	0.0045
	(0.0118)	(0.0572)	(0.0118)
Block FE	Yes	Yes	Yes
Year-month FE	Yes	Yes	Yes
municipality×Year FE	No	Yes	Yes
Observations	467,034	22,417	27,554

Notes: Violence index ranges 0–3. Near closed metro = 1 if within 500m of a closed station. Dependent variable is log price for Residential and Commercial, and $\ln(\text{UF}/m^2)$ for Rents. Standard errors clustered at the block level for Residential and Commercial, and at the manzana level for Rents. $^{*}p < 0.10$, $^{**}p < 0.05$, $^{***}p < 0.01$.

5.3 Transaction volumes

Table 5 examines whether violence exposure affected residential market activity[7]. The dependent variable in Panel A is $\ln(1+n)$, where n denotes the number of residential transactions in a block-quarter. Column (1) reports a two-way fixed effects specification with a small, statistically significant coefficient. Once municipality-by-year fixed effects are included in Column (2), the estimate shrinks toward zero and becomes statistically indistinguishable from zero. Column (3) shows that this null result also holds when allowing the effect of violence exposure to vary across post-shock phases.

Taken together with the price results, these estimates provide little support for differential declines in residential trading activity in more exposed blocks. Residential prices fall in moderately and highly exposed areas, yet transaction volumes do not differentially decline once comuna-by-year shocks are absorbed. Event-study estimates for transaction volumes in Figure A.4 corroborate the absence of meaningful differential changes across exposure groups.

Regarding commercial properties, the limited precision of commercial price estimates makes market activity a particularly informative margin. Table 5 therefore examines transaction volumes, separating participation from transaction intensity. Panel A reports effects on the probability that a block-quarter has any commercial transaction. Panel B reports PPML estimates for transaction counts with an offset for commercial stock, which can be interpreted as effects on transaction rates conditional on the local stock of commercial properties.

Panel A shows that violence exposure reduces market participation. In the baseline specification with municipality-by-year fixed effects, each one-unit increase in the violence index lowers the probability of any commercial transaction by 0.42 percentage points. Relative to a baseline transaction probability of 2.98% in the control group, this implies a sizable decline

[7] Complete tables: Residential is in Table A.5, Commercial in Table A.6, and Rents in A.7.

in participation in high-exposure blocks.[8] The estimates are negative across phases, with statistically significant declines in Phase 1 and Phase 3. Panel B yields imprecise estimates for transaction rates, with no robust evidence of changes in conditional intensity. Overall, the evidence is consistent with commercial adjustment operating primarily through reduced participation and market thinning rather than through a clear decline in transaction rates among blocks that remain active. Figure A.5 reports complementary event-study evidence.

Finally, I examine rental listings as a complementary measure of market activity. Violence exposure increases the probability that a block-quarter has any listing during the metro-closure and COVID phases, while the number of listings conditional on being active declines in the post-normalization phase. This pattern is consistent with reallocation of listing activity across space and time, and it reinforces the interpretation that the post-2022 adjustment is not driven solely by short-run disruptions.

Overall, the evidence across outcomes points to persistent residential price discounts in moderately and highly exposed blocks without commensurate declines in residential market activity. In contrast, commercial market adjustment is concentrated on the participation margin, consistent with market thinning and selection in the transacting sample.

[8] Computed as $100 \times (3 \times 0.0042)/0.0298$.

Table 5: Summary of Difference-in-Differences Estimates for Market Activity

	(1) TWFE	(2) + mun. × Year	(3) By Phase
Panel A. Residential Transaction Volumes (			
A.1 OLS N=1,258,426			
Post × Viol. index	-0.0082***	-0.0017	
Viol. index × Phase 1			-0.0027
Viol. index × Phase 2			-0.0017
Viol. index × Phase 3			-0.0012
A.2 PPML N=998,528			
Post × Viol. index	0.0626**	0.0149	
Viol. index × Phase 1			0.0398
Viol. index × Phase 2			-0.0069
Viol. index × Phase 3			0.0199
Panel B. Commercial Transaction Volumes			
B.1 OLS N=341,765			
Post × Viol. index	-0.0047***	-0.0037***	
Viol. index × Phase 1			-0.0054***
Viol. index × Phase 2			-0.0025*
Viol. index × Phase 3			-0.0035***
B.2 PPML N=95,410			
Post × Viol. index	0.0742	0.0643	
Viol. index × Phase 1			0.0781
Viol. index × Phase 2			0.0202
Viol. index × Phase 3			0.0927
Panel C. Rental Listings Volumes			
C.1 OLS N=1,258,426			
Post × Viol. index	0.0013***	0.0014***	
Viol. index × Phase 1			0.0029***
Viol. index × Phase 2			0.0018***
Viol. index × Phase 3			0.0002
C.2 PPML N=70,350			
Post × Viol. index	-0.0227	-0.0347	
Viol. index × Phase 1			0.0226
Viol. index × Phase 2			-0.0509
Viol. index × Phase 3			-0.1453***
Manzana FE	Yes	Yes	Yes
Event-quarter FE	Yes	Yes	Yes
mun. × Year FE	No	Yes	Yes

Phases. Phase 1 (metro closure) is Oct 2019–Sep 2020. Phase 2 (COVID/transition) is Oct 2020–Sep 2022. Phase 3 (post-normalization) is Oct 2022 onward.
Significance. *** $p < 0.01$, ** $p < 0.05$, * $p < 0.10$.
Sample size. In PPML panels, N varies slightly across columns due to the estimation sample.

6 Mechanisms and heterogeneity

This section documents heterogeneity patterns that are informative about mechanisms. These results complement the core identification evidence in Section 5 but are not designed to separately identify causal channels on their own.

6.1 Heterogeneity by centrality

I examine spatial heterogeneity by distance to Plaza Italia, used as a proxy for the CBD. Table 6 reports estimates by distance rings for the post-normalization period. Residential effects are largest within 2 km of the CBD, where prices fall by 2.9% per unit of violence intensity and rents by 3.6%. Estimates remain negative in several outer rings, which is consistent with unrest affecting secondary centers and transport corridors outside the core. The non-monotonic pattern across discrete bins suggests caution in interpreting the cutoffs as sharp thresholds.

Table 6: Violence Effects by Distance to CBD in Phase 3

	Residential (Sales)	Commercial (Sales)	Residential (Rents)
0–2km	-0.029^{***}	-0.045^{*}	-0.036^{***}
	(0.008)	(0.026)	(0.012)
2–5km	-0.017	-0.018	-0.035^{***}
	(0.012)	(0.026)	(0.009)
5–10km	-0.019	0.072	-0.004
	(0.017)	(0.062)	(0.016)
>10km	-0.022^{***}	0.131^{**}	0.011
	(0.009)	(0.054)	(0.013)
FE (unit / time / municipality×year)	Yes	Yes	Yes
Observations	443,593	20,947	27,554

Notes. Distance is measured from Plaza Italia. Coefficients are per unit of violence intensity (0–3) in the post-normalization period (Phase 3). The dependent variable is log price for sales and $\ln(\text{UF}/m^2)$ for rents. Standard errors are clustered at the block level. $^{*}p < 0.10$, $^{**}p < 0.05$, $^{***}p < 0.01$.

6.2 Heterogeneity by socioeconomic status

Table 7 examines heterogeneity by neighborhood socioeconomic status (GSE). Residential sales effects are concentrated in medium- and high-GSE areas, while low-GSE areas show no discernible response. For rents, the largest declines occur in high-GSE areas. This pattern is consistent with higher-income households being more responsive to perceived safety risks and having greater residential mobility. At the same time, alternative explanations related to correlated centrality and amenity gradients cannot be fully ruled out.

Table 7: Violence Effects by Socioeconomic Status in Phase 3

	Residential (Sales)	Commercial (Sales)	Residential (Rents)
Low GSE	0.0014	0.0257	0.0005
	(0.0105)	(0.0804)	(0.0231)
Medium GSE	-0.0298^{***}	0.0389	0.0030
	(0.0091)	(0.0419)	(0.0109)
High GSE	-0.0209^{**}	-0.0217	-0.0333^{***}
	(0.0089)	(0.0254)	(0.0086)
FE (block / year-month / municipality×year)	Yes	Yes	Yes
Observations	443,593	20,947	27,440

Notes. Results are reported for the post-normalization period (Phase 3). Coefficients are per unit of violence intensity (0–3). The dependent variable is log price for sales and $\ln(\text{UF}/m^2)$ for rents. Standard errors are clustered at the block level. $^{*}p < 0.10$, $^{**}p < 0.05$, $^{***}p < 0.01$.

6.3 Prior crime conditions

Finally, I assess whether the estimated price response varies with baseline neighborhood safety. Using police quadrant data matched to blocks, I examine whether price effects differ by pre-period crime levels and their interaction with neighborhood socioeconomic status. These analyses rely on a smaller matched sample and are reported in Table 8 and Table A.12. The results indicate larger price declines in higher-crime areas, consistent with unrest reinforcing pre-existing safety concerns. The interaction patterns suggest that baseline crime and socioeconomic composition jointly shape the magnitude of the response.

Table 8: Residential Violence Effects by Prior Crime

	(1) Low vs High Crime	(2) Crime × GSE
Violence × Low Crime (2018)	-0.0140^{*}	
	(0.0084)	
Violence × High Crime (2018)	-0.0215^{***}	
	(0.0065)	
Violence × Low Crime × High GSE		-0.0245
		(0.0156)
Violence × Low Crime × Low GSE		-0.0090
		(0.0093)
Violence × High Crime × High GSE		-0.0186^{**}
		(0.0090)
Violence × High Crime × Low GSE		-0.0256^{***}
		(0.0080)
Block FE / Year-month FE / municipality×Year FE	Yes	Yes
Observations	449,001	449,001

Notes. Estimates are for the post-normalization period. Standard errors are clustered at the block level. * $p < 0.10$, ** $p < 0.05$, *** $p < 0.01$.

7 Robustness

This section evaluates the sensitivity of the main residential price result to alternative specifications, sample restrictions, and inference procedures. I consider six sets of checks. First, I allow for flexible time shocks correlated with centrality and commercial activity. Second, I restrict the sample to observations near the violence boundary. Third, I examine pre-trends and placebo timing. Fourth, I estimate repeat-sales specifications with property fixed effects. Fifth, I assess spatial dependence in inference. Sixth, I vary the threshold used to define treatment channels based on proximity to closed metro stations. Across these exercises, the Phase 3 estimate remains negative and is typically statistically significant. Detailed results are reported in the Appendix.

A concern is that the baseline estimate reflects time-varying shocks correlated with centrality or commercial intensity rather than violence exposure. I address this by replacing year-month fixed effects with flexible interactions that allow month shocks to differ by distance-to-CBD bins and commercial-density bins. Appendix Table A.16 shows that the Phase 3 coefficient remains negative under these saturated controls. Relative to the baseline

Phase 3 estimate of -0.020, the coefficient attenuates to -0.015 with CBD$\times$month effects, -0.018 with commercial-density$\times$month effects, and -0.014 when both sets of interactions are included. The persistence of negative estimates indicates that the result is not driven solely by centrality- or commerce-specific shocks.

I also probe sensitivity to restricting the sample to observations near the violence boundary. Very narrow bandwidths (250–500m) yield imprecise estimates, consistent with limited power in highly local samples and with the fact that $V = 1$ exposure dominates in narrow rings. For broader windows, the effect re-emerges, with estimates around -0.017 at 1,000m and 1,500m (Appendix Table **??**). These exercises are local sample restrictions rather than a regression discontinuity design, but they suggest that the baseline effect is not driven by observations far from the boundary.

Identification requires the absence of differential pre-trends correlated with violence exposure. I test the joint null that all pre-period event-study coefficients equal zero. The Wald test fails to reject (Appendix Table A.17), and pre-period coefficients are visually flat in Figure 5. To assess whether the design mechanically produces effects at other dates, I implement placebo tests that assign fake shock months in the pre-period. Appendix Figure A.11 reports 12 placebo estimates (April 2018–March 2019). Placebo coefficients are centered near zero, lie in the range $[-0.005, 0.011]$, and none approaches the Phase 3 estimate of approximately -0.02.

Results might also be driven by the immediate surroundings of Plaza Italia, the symbolic center of protests. I implement donut tests that exclude transactions within progressively larger radii around Plaza Italia. The Phase 3 coefficient is similar when excluding up to 1km (Appendix Table A.19). Similar stability holds for donuts around secondary epicenters, including Puente Alto and Maipú, as well as around the nearest epicenter to each transaction (Appendix Table A.20).

To address time-invariant unobserved property quality, I estimate repeat-sales specifications on properties sold both before and after the shock, including property fixed effects. The

Phase 3 coefficient is larger (-0.041, s.e. 0.011) than the baseline block fixed-effect estimate (Appendix Table A.21). Given the substantial sample restriction and the scope for selection into repeat sales, I interpret this pattern as suggestive evidence of heterogeneity rather than as a replacement for the population-average estimate.

Finally, I assess sensitivity to spatial correlation using Conley standard errors with varying distance cutoffs. Point estimates are unchanged, and standard errors using 1–2km cutoffs are comparable to block clustering (Appendix Table A.22). I also vary the metro proximity threshold used to define treatment channels, from 300m to 800m. The *Violence Only* Phase 3 effect remains stable around -0.018 across thresholds (Appendix Figure A.12). The *Both* coefficient is more negative at tighter thresholds and attenuates as the radius expands, consistent with joint exposure being most salient immediately around closed stations.

8 Conclusion

This paper studies how concentrated episodes of urban violence affect real estate markets, using the October 2019 social unrest in Santiago, Chile. Combining georeferenced prosecutorial incident data with the universe of property transactions and rental listings, I document four main findings.

First, residential price effects display a threshold pattern and persist around five years after the onset of unrest. In the post-normalization period, properties in moderate- and high-efxposure areas ($V = 2$ and $V = 3$) experience price declines of roughly 5–6%, while low-exposure areas ($V = 1$) show small and statistically indistinguishable effects. The nonlinear response, together with dynamics that strengthen rather than fade over time, is consistent with a reputational mechanism in which sufficiently salient violence durably affects perceived neighborhood quality. Rental markets display a related pattern, with declines concentrated in higher-intensity locations and strengthening over time, supporting the interpretation that the shock altered local demand conditions rather than generating a purely transitory disruption.

This nonlinear response, together with dynamics that strengthen rather than fade over time, is consistent with persistent disamenity and perceived risk, although alternative mechanisms related to local activity and amenity changes cannot be fully ruled out.

Second, the residential response is more closely linked to violence exposure than to metro-accessibility losses. The *Violence Only* channel shows persistent declines, while the *Metro Only* channel is close to zero. Triple-difference estimates likewise indicate that proximity to closed stations does not explain the residential price response once the model incorporates flexible time-varying local controls.

Third, commercial real estate adjusts primarily through market participation rather than observed transaction prices. I find large and persistent declines in the probability of any commercial transaction in more violent areas. This extensive-margin contraction implies market thinning and raises concerns about selection among the transacting sample, helping to rationalize why hedonic price estimates for commercial properties are imprecise.

Fourth, heterogeneity patterns show larger residential effects in medium- and high-socioeconomic-status neighborhoods and near the city center. This is consistent with higher-income households being more responsive to perceived safety risks and having greater residential mobility. At the same time, alternative channels related to sorting, local economic activity, and amenity change cannot be fully ruled out.

The paper contributes to several strands of the literature. It extends work on riots and civil unrest by providing evidence from a major Latin American city using high-coverage administrative data and fine spatial exposure measures. It adds to the crime capitalization literature by studying an acute episode of concentrated violence rather than changes in ambient crime rates, and by tracing dynamics over a multi-year horizon. Methodologically, it illustrates how combining channel classification with a triple-difference decomposition can help address confounding when violence exposure and accessibility shocks are spatially correlated.

Several limitations warrant acknowledgment. Although the patterns are consistent with reputational scarring, the data cannot definitively distinguish stigma from other mechanisms, including changes in local business activity, population sorting, or unobserved amenity shifts correlated with violence exposure. The commercial price analysis is constrained by sample size and by selection from non-trading, which motivates greater reliance on transaction-volume outcomes. The COVID-19 pandemic complicates interpretation during 2020–2022, but the post-normalization period provides a cleaner setting to evaluate persistence after metro service is restored and major restrictions have ended.

Overall, the results imply that the economic footprint of violence can persist well beyond the restoration of infrastructure and the end of acute disruptions. The concentration of effects in higher-SES and central neighborhoods suggests that the incidence of capitalization may fall disproportionately on households with higher willingness to pay for perceived safety. At the same time, muted effects in low-SES areas could reflect lower marginal valuations of safety, tighter housing constraints, or compositional adjustments that are not fully captured in transaction data.

More broadly, the persistence of effects years after the shock suggests that concentrated violence can durably alter urban structure. For cities that face recurrent episodes of unrest, understanding these medium- and long-run consequences, and identifying interventions that reduce reputational scarring and support recovery in affected neighborhoods, remains an important agenda for research and policy.

References

Abadie, Alberto and Sofia Dermisi, "Is terrorism eroding agglomeration economies in Central Business Districts? Lessons from the office real estate market in downtown Chicago," *Journal of Urban Economics*, 9 2008, *64* (2), 451–463.

Agostini, Claudio A. and Gaston Palmucci, "Capitalización Heterogénea de un Bien Semipúblico: El Metro de Santiago," *Cuadernos de economía*, 2008, *45* (131), 105–128.

Araya, Martín Rosas, "Calculating Socio Material Territorial Index [R package ismtchile version 2.1.5]," *CRAN: Contributed Packages*, 7 2023.

Avendaño, Octavio, "ESTALLIDO SOCIAL EN CHILE: LOS DILEMAS POLÍTICOS DESDE OCTUBRE DEL 2019," *Política. Revista de Ciencia Política*, 12 2019, *57* (2), 105–119.

Besley, Timothy and Hannes Mueller, "Estimating the Peace Dividend: The Impact of Violence on House Prices in Northern Ireland," *American Economic Review*, 2012, *102* (2), 810–33.

Braakmann, Nils, "The link between crime risk and property prices in England and Wales: Evidence from street-level data," *Urban Studies*, 6 2017, *54* (8), 1990–2007.

Callaway, Brantly and Pedro H.C. Sant'Anna, "Difference-in-Differences with multiple time periods," *Journal of Econometrics*, 12 2021, *225* (2), 200–230.

Ceccato, Vania and Mats Wilhelmsson, "Do crime hot spots affect housing prices?," *Nordic Journal of Criminology*, 1 2020, *21* (1), 84–102.

Ceccato, Vânia and Mats Wilhelmsson, "The Impact Of Crime On Apartment Prices: Evidence From Stockholm, Sweden," *Geografiska Annaler, Series B: Human Geography*, 3 2011, *93* (1), 81–103.

COES, “Protest Events Dataset 2008-2020,” 2020.

Collins, William J and Robert A Margo, “The Economic Aftermath of the 1960s Riots in American Cities: Evidence from Property Values,” *Journal of Economic History*, 12 207, (67), 849–883.

Cox, Loreto, Ricardo González, and Carmen Le Foulon, “The 2019 Chilean Social Upheaval: A Descriptive Approach,” *Journal of Politics in Latin America*, 4 2024, *16* (1), 68–89.

Davis, Donald R. and David E. Weinstein, “Bones, Bombs, and Break Points: The Geography of Economic Activity,” *American Economic Review*, 12 2002, *92* (5), 1269–1289.

de Chaisemartin, Clément and Xavier D’Haultfœuille, “Two-Way Fixed Effects Estimators with Heterogeneous Treatment Effects,” *American Economic Review*, 9 2020, *110* (9), 2964–96.

Fiscalia Nacional, “Informe Estallido Social,” Technical Report, Ministerio Publico 2025.

Gibbons, Steve, “The costs of urban property crime,” *Economic Journal*, 11 2004, *114* (499), F441–F463.

Gonzalez, Ricardo and Carmen Le Foulon Morán, “The 2019–2020 Chilean protests: A first look at their causes and participants,” *International Journal of Sociology*, 5 2020, *50* (3), 227–235.

Gourley, Patrick, “Social Stigma and Asset Value,” *Southern Economic Journal*, 1 2019, *85* (3), 919–938.

Haig, Christian Stirling, Katherine Schmidt, and Samuel Brannen, “The Age of Mass Protests: Understanding an Escalating Global Trend,” 2020.

Klimova, Anastasia and Adrian D. Lee, "Does a nearby murder affect housing prices and rents? The case of Sydney," *Economic Record*, 2014, *90* (S1), 16–40.

Kourtis, Eleftherios, Panayiotis Curtis, and Michael Kourtis, "Spatial Differentiation of Urban Property Prices as a Repercussion in the Aftermath of a Civil Disorder Incident: The 2011 London Case," *International Journal of Finance, Insurance and Risk Management*, 2020, *10* (4), 3–24.

Lens, Michael C and Rachel Meltzer, "IS CRIME BAD FOR BUSINESS? CRIME AND COMMERCIAL PROPERTY VALUES IN NEW YORK CITY *," *JOURNAL OF REGIONAL SCIENCE*, 2016, *56* (3), 442–470.

Linden, Leigh and Jonah E. Rockoff, "Estimates of the Impact of Crime Risk on Property Values from Megan's Laws," *American Economic Review*, 2008, *98* (3), 1103–27.

Metro de Santiago, "Memoria Anual," 2020.

Sasse, Lea, "Chile Despertó-The Reasons for the Mass Protests in Chile Contact," 2019.

Thaler, Richard, "A note on the value of crime control: Evidence from the property market," *Journal of Urban Economics*, 1 1978, *5* (1), 137–145.

Table A.1: Summary Statistics: Control vs. Violence-Exposed Areas (Pre-Period)

	Control		Treated			
	Mean	SD	Mean	SD	Diff.	p-value
Panel A: Residential Transactions						
Price (UF/m^2)	44.58	26.48	51.97	26.08	7.39	0.000***
Total Price (UF)	3142.44	3566.86	3366.38	2503.72	223.95	0.000***
Construction (m^2)	65.28	38.79	64.90	30.87	-0.38	0.028**
Year Built	2003.13	19.34	1999.45	20.92	-3.68	0.000***
Apartment (=1)	0.64	0.48	0.70	0.46	0.07	0.000***
Observations	129,161		51,278			
Panel B: Commercial Transactions						
Price (UF/m^2)	67.36	40.98	63.72	36.85	-3.64	0.000***
Total Price (UF)	7572.94	24777.92	10043.31	26647.96	2470.37	0.000***
Construction (m^2)	156.11	774.13	198.46	874.37	42.35	0.018**
Year Built	1998.75	26.51	1988.38	29.79	-10.37	0.000***
Office (=1)	0.62	0.49	0.65	0.48	0.02	0.020**
Observations	5,339		3,675			
Panel C: Block Characteristics						
Residential Stock	40.59	89.22	49.56	101.20	8.97	0.000***
Commercial Stock	1.32	13.54	3.83	28.34	2.51	0.000***
Distance to Metro (m)	4193.53	5773.13	1526.75	1607.82	-2666.78	0.000***
Pop. Density (per/ha)	201.22	196.51	193.25	166.53	-7.97	0.000***
Population 2017	134.70	188.33	141.46	198.82	6.76	0.002***
GSE Level	1.57	0.67	1.77	0.65	0.19	0.000***
Avg. Quarterly Res. Txn	0.45	3.74	0.56	2.51	0.11	0.000***
Avg. Quarterly Com. Txn	0.02	0.54	0.04	0.43	0.02	0.000***
Avg. Quarterly Rent Listings	0.01	0.17	0.03	0.19	0.02	0.000***
Blocks	34,060		10,639 (23.8%)			
Panel D: Rental Listings						
Rent (UF/m^2)	0.32	0.10	0.31	0.09	-0.01	0.032**
Rent (UF)	29.05	15.57	22.19	10.38	-6.86	0.000***
Size (m^2)	96.55	50.40	75.79	35.76	-20.76	0.000***
Bedrooms	2.36	0.91	2.06	0.86	-0.30	0.000***
Bathrooms	2.08	0.85	1.79	0.67	-0.29	0.000***
Observations	3,858		2,570			

Notes: Pre-period defined as Oct 2017–Sep 2019 (event_time< 0). Treated blocks have violence index ≥ 1. Stars indicate significance: * p<0.10, ** p<0.05, *** p<0.01.

Appendix

Appendix: Additional Tables

Table A.2: Difference-in-Differences Estimates for Residential Prices

	(1) TWFE	(2) + municipality×Year	(3) By Phase	(4) By Phase and V_b
Post × Viol. index	-0.020***	-0.010*		
	(0.004)	(0.005)		
Viol. index × Phase 1			-0.006	
			(0.005)	
Viol. index × Phase 2			-0.007	
			(0.006)	
Viol. index × Phase 3			-0.020***	
			(0.006)	
Phase 1 × $V = 1$				-0.014
				(0.012)
Phase 1 × $V = 2$				-0.034**
				(0.017)
Phase 1 × $V = 3$				-0.005
				(0.014)
Phase 2 × $V = 1$				-0.013
				(0.011)
Phase 2 × $V = 2$				-0.030
				(0.020)
Phase 2 × $V = 3$				-0.010
				(0.019)
Phase 3 × $V = 1$				-0.009
				(0.014)
Phase 3 × $V = 2$				-0.051***
				(0.018)
Phase 3 × $V = 3$				-0.059***
				(0.018)
Block FE	Yes	Yes	Yes	Yes
Year-month FE	Yes	Yes	Yes	Yes
municipality×Year FE	No	Yes	Yes	Yes
Observations	467,034	467,034	467,034	467,034
R^2	0.85215	0.85364	0.85365	0.85367
Within R^2	0.27537	0.27560	0.27567	0.27573

Notes. Dependent variable is ln(price). Standard errors clustered at the block level in parentheses. Columns (2)–(4) include municipality-by-year fixed effects. Column (3) is relative to the omitted pre-period. Column (4) is relative to the omitted category (pre, $V = 0$).

Phases. Phase 1 (metro closure) is Oct 2019–Sep 2020. Phase 2 (COVID/transition) is Oct 2020–Sep 2022. Phase 3 (post-normalization) is Oct 2022 onward.

Significance. *** $p < 0.01$, ** $p < 0.05$, * $p < 0.10$.

Table A.3: Difference-in-Differences Estimates: Commercial Prices

	(1) TWFE	(2) + municipality×Year	(3) By Phase	(4) By Phase and V_b
Post × Viol. index	-0.016	0.010		
	(0.014)	(0.016)		
Viol. index × Phase 1			0.012	
			(0.019)	
Viol. index × Phase 2			0.025	
			(0.022)	
Viol. index × Phase 3			-0.014	
			(0.021)	
Phase 1 × $V = 1$				-0.044
				(0.078)
Phase 1 × $V = 2$				0.053
				(0.068)
Phase 1 × $V = 3$				0.034
				(0.056)
Phase 2 × $V = 1$				0.075
				(0.056)
Phase 2 × $V = 2$				0.011
				(0.069)
Phase 2 × $V = 3$				0.075
				(0.065)
Phase 3 × $V = 1$				0.015
				(0.061)
Phase 3 × $V = 2$				-0.039
				(0.068)
Phase 3 × $V = 3$				-0.048
				(0.062)
Block FE	Yes	Yes	Yes	Yes
Year-month FE	Yes	Yes	Yes	Yes
municipality×Year FE	No	Yes	Yes	Yes
Observations	22,417	22,417	22,417	22,417
R^2	0.85671	0.86278	0.86284	0.86292
Within R^2	0.61260	0.61335	0.61351	0.61374

Notes: Dependent variable is ln(price). Standard errors clustered at the block level in parentheses. Columns (2)–(4) include municipality-by-year fixed effects. Column (3) is relative to the omitted pre-period. Column (4) is relative to the omitted category (pre, $V = 0$).

Phases: Phase 1 (Metro closure) = Oct 2019–Sep 2020; Phase 2 (COVID/transition) = Oct 2020–Sep 2022; Phase 3 (Post-normalization) = Oct 2022 onward.

Significance: *** $p < 0.01$, ** $p < 0.05$, * $p < 0.10$.

Table A.4: Difference-in-Differences Estimates: Rental Asking Rents (UF/m^2)

	(1) TWFE	(2) + municipality×Year	(3) By Phase	(4) By Phase and V_b
Post × Viol. index	-0.018***	-0.018***		
	(0.004)	(0.005)		
Viol. index × Phase 1			-0.015**	
			(0.006)	
Viol. index × Phase 2			-0.018***	
			(0.006)	
Viol. index × Phase 3			-0.028***	
			(0.007)	
Phase 1 × $V = 1$				-0.023
				(0.018)
Phase 1 × $V = 2$				-0.022
				(0.017)
Phase 1 × $V = 3$				-0.042**
				(0.020)
Phase 2 × $V = 1$				-0.017
				(0.017)
Phase 2 × $V = 2$				-0.015
				(0.016)
Phase 2 × $V = 3$				-0.057***
				(0.019)
Phase 3 × $V = 1$				-0.009
				(0.017)
Phase 3 × $V = 2$				-0.040**
				(0.020)
Phase 3 × $V = 3$				-0.088***
				(0.023)
Block FE	Yes	Yes	Yes	Yes
Year-month FE	Yes	Yes	Yes	Yes
municipality×Year FE	No	Yes	Yes	Yes
Observations	31,739	27,554	27,554	27,554
R^2	0.60119	0.62555	0.62566	0.62580
Within R^2	0.24111	0.24080	0.24101	0.24130

Notes: Dependent variable is ln(UF/m^2) for asking rents. Standard errors clustered at the block level in parentheses. Columns (2)–(4) include municipality-by-year fixed effects. Column (3) is relative to the omitted pre-period. Column (4) is relative to the omitted category (pre, $V = 0$).
Phases: Phase 1 (Metro closure) = Oct 2019–Sep 2020; Phase 2 (COVID/transition) = Oct 2020–Sep 2022; Phase 3 (Post-normalization) = Oct 2022 onward.
Significance: *** $p < 0.01$, ** $p < 0.05$, * $p < 0.10$.

Table A.5: Residential Transaction Volumes

	(1) TWFE	(2) + Comuna×Year	(3) By Phase
Panel A. OLS with $\ln(1 + n_{res})$			
Post × Viol. index	-0.0082***	-0.0017	
	(0.0013)	(0.0014)	
Viol. index × Phase 1			-0.0027
			(0.0017)
Viol. index × Phase 2			-0.0017
			(0.0016)
Viol. index × Phase 3			-0.0012
			(0.0016)
Panel B. PPML for transaction counts			
Post × Viol. index	0.0626**	0.0149	
	(0.0287)	(0.0310)	
Viol. index × Phase 1			0.0398
			(0.0495)
Viol. index × Phase 2			-0.0069
			(0.0375)
Viol. index × Phase 3			0.0199
			(0.0474)
Manzana FE	Yes	Yes	Yes
Event-quarter FE	Yes	Yes	Yes
Comuna×Year FE	No	Yes	Yes
Observations (Panel A)	1,258,426	1,258,426	1,258,426
Observations (Panel B)	998,528	998,464	998,464

Notes. Unit of observation is manzana-by-quarter. Panel A reports OLS with dependent variable $\ln(1 + n_{\text{res}})$. Panel B reports PPML for residential transaction counts. Standard errors are clustered at the manzana level.

Phases. Phase 1 (metro closure) is Oct 2019–Sep 2020. Phase 2 (COVID/transition) is Oct 2020–Sep 2022. Phase 3 (post-normalization) is Oct 2022 onward.

Significance. *** $p < 0.01$, ** $p < 0.05$, * $p < 0.10$.

Table A.6: Commercial Transaction Volumes

	(1) TWFE	(2) + municipality×Year	(3) By Phase
Panel A: Extensive margin (Any commercial transaction)			
Post × Viol. index	-0.0047***	-0.0037***	
	(0.0010)	(0.0011)	
Viol. index × Phase 1			-0.0054***
			(0.0015)
Viol. index × Phase 2			-0.0025*
			(0.0013)
Viol. index × Phase 3			-0.0035***
			(0.0013)
Panel B: Intensive margin (PPML transaction count)			
Post × Viol. index	0.0742	0.0643	
	(0.0527)	(0.0789)	
Viol. index × Phase 1			0.0781
			(0.1013)
Viol. index × Phase 2			0.0202
			(0.0801)
Viol. index × Phase 3			0.0927
			(0.0943)
Manzana FE	Yes	Yes	Yes
Event-quarter FE	Yes	Yes	Yes
municipality×Year FE	No	Yes	Yes
Observations (Panel A)	341,765	341,765	341,765
Observations (Panel B)	95,410	95,206	95,206

Notes: Panel A is an LPM with dependent variable $\mathbb{1}\{n_{\text{com}} > 0\}$. Panel B reports PPML for commercial transaction counts. Standard errors clustered at the manzana level.

Phases: Phase 1 (Metro closure) = Oct 2019–Sep 2020; Phase 2 (COVID/transition) = Oct 2020–Sep 2022; Phase 3 (Post-normalization) = Oct 2022 onward.

Significance: *** $p < 0.01$, ** $p < 0.05$, * $p < 0.10$.

Table A.7: Rental Listings Volumes

	(1) TWFE	(2) + municipality×Year	(3) By Phase
Panel A: Extensive margin (Any rental listing)			
Post × Viol. index	0.0013***	0.0014***	
	(0.0004)	(0.0004)	
Viol. index × Phase 1			0.0029***
			(0.0006)
Viol. index × Phase 2			0.0018***
			(0.0005)
Viol. index × Phase 3			0.0002
			(0.0004)
Panel B: Intensive margin (PPML listing count)			
Post × Viol. index	-0.0227	-0.0347	
	(0.0287)	(0.0343)	
Viol. index × Phase 1			0.0226
			(0.0395)
Viol. index × Phase 2			-0.0509
			(0.0380)
Viol. index × Phase 3			-0.1453***
			(0.0468)
Manzana FE	Yes	Yes	Yes
Event-quarter FE	Yes	Yes	Yes
municipality×Year FE	No	Yes	Yes
Observations (Panel A)	1,258,426	1,258,426	1,258,426
Observations (Panel B)	70,350	69,509	69,509

Notes: Panel A is an LPM with dependent variable $\mathbb{1}\{n_{\text{rent}} > 0\}$. Panel B reports PPML for the number of rental listings. Standard errors clustered at the manzana level.

Phases: Phase 1 (Metro closure) = Oct 2019–Sep 2020; Phase 2 (COVID/transition) = Oct 2020–Sep 2022; Phase 3 (Post-normalization) = Oct 2022 onward.

Significance: *** $p < 0.01$, ** $p < 0.05$, * $p < 0.10$.

Table A.8: Covariate Balance: Event Study Summary

	Mean Coefficient		% Significant	
Covariate	Pre	Post	Pre	Post
Residential				
Apartment (=1)	0.007	0.014	12.5%	52.4%
Log Construction Size	0.005	-0.011	0.0%	9.5%
Log Distance to Metro	-0.002	-0.001	0.0%	0.0%
Log Year Built	0.000	0.000	0.0%	9.5%
Commercial				
Log Construction Size	-0.042	-0.119	0.0%	9.5%
Log Distance to Metro	0.017	0.035	0.0%	9.5%
Log Year Built	0.001	0.001	0.0%	4.8%
Office (=1)	0.008	0.004	0.0%	0.0%
Rents				
Bathrooms	-0.014	-0.058	0.0%	5.9%
Bedrooms	0.036	0.002	0.0%	0.0%
Log Distance to Metro	0.009	0.003	0.0%	0.0%
Log Unit Size	0.019	-0.008	0.0%	0.0%

Notes: Event study coefficients from regression of each covariate on treated × quarter indicators with block and year-month fixed effects. % Significant = share of quarters with $|t| > 1.96$.

Table A.9: Triple-Difference Coefficients by Phase

	Residential	Commercial
Violence index		
Phase 1	−0.0051	0.0008
	(0.0052)	(0.0197)
Phase 2	−0.0045	0.0177
	(0.0064)	(0.0238)
Phase 3	−0.0175***	−0.0274
	(0.0060)	(0.0222)
Near closed metro		
Phase 1	−0.0054	−0.0901
	(0.0211)	(0.1724)
Phase 2	0.0019	−0.2559
	(0.0198)	(0.1580)
Phase 3	−0.0083	−0.3291**
	(0.0247)	(0.1607)
Violence × Near metro		
Phase 1	−0.0030	0.1204
	(0.0108)	(0.0798)
Phase 2	−0.0204	0.1261
	(0.0140)	(0.0800)
Phase 2	−0.0133	0.1945**
	(0.0136)	(0.0786)
Block FE	Yes	Yes
Year-month FE	Yes	Yes
municipality×Year FE	Yes	Yes
Observations	467,034	22,417

Notes: Standard errors clustered at the block level. * $p < 0.10$, ** $p < 0.05$, *** $p < 0.01$.

Table A.10: Violence × CBD Distance

	Residential	Commercial
Violence index × Phase 3	−0.0202***	0.0205
	(0.0062)	(0.0242)
Violence × Distance to CBD (std.) × Phase 3	−0.0011	0.0502***
	(0.0036)	(0.0174)
Block FE	Yes	Yes
Year-month FE	Yes	Yes
municipality×Year FE	Yes	Yes
Observations	467,034	22,417

Notes: "Distance to CBD (std.)" is standardized (mean 0, SD 1). Standard errors clustered at the block level. * $p < 0.10$, ** $p < 0.05$, *** $p < 0.01$.

Table A.11: Commercial: Violence Effects by Prior Crime

	Commercial
Violence × Low Crime (2018)	0.0386
	(0.0647)
Violence × High Crime (2018)	−0.0136
	(0.0211)
Block FE / Year-month FE / municipality×Year FE	Yes
Observations	22,240

Notes: Post-normalization period. Standard errors clustered at the block level. * $p < 0.10$, ** $p < 0.05$, *** $p < 0.01$.

Table A.12: Violence Effects by Prior Crime × Socioeconomic Status

	Low crime×High GSE	Low crime×Low GSE	High crime×High GSE	High crime×Low GSE
Phase 1	−0.0003	−0.0034	0.0014	-0.0122^{*}
	(0.0122)	(0.0087)	(0.0054)	(0.0071)
Phase 2	−0.0100	0.0032	-0.0102^{*}	−0.0086
	(0.0094)	(0.0114)	(0.0061)	(0.0085)
Phase 3	−0.0245	−0.0090	-0.0186^{**}	-0.0256^{***}
	(0.0156)	(0.0093)	(0.0090)	(0.0080)
Block FE	Yes			
Year-month FE	Yes			
Mun.×Year FE	Yes			
Obs.	449,001			

Notes: Dependent variable is log price. Crime groups are defined using the median of 2018 quadrant-level crime rates. GSE is measured at the block (manzana) level. Standard errors clustered at the block level. Significance: $^{*}p < 0.10$, $^{**}p < 0.05$, $^{***}p < 0.01$.

Table A.13: Which Types of Prior Crime Amplify Violence Effects? (Residential)

	Log price
Violence index × Phase 3	-0.0178^{***}
	(0.0065)
Violence × Robbery (std.) × Phase 3	-0.0085^{**}
	(0.0043)
Violence × Theft (std.) × Phase 3	−0.0052
	(0.0038)
Violence × Drug (std.) × Phase 3	0.0120^{**}
	(0.0048)
Block FE / Year-month FE / municipality×Year FE	Yes
Observations	449,001

Notes: Crime rates standardized (mean 0, SD 1). Standard errors clustered at the block level. * $p < 0.10$, ** $p < 0.05$, *** $p < 0.01$.

Table A.14: Crime Rates Before and After the 2019 Unrest (Cuadrante Level)

Group	Crime rate 2018	Crime rate 2023	Δ
No violence exposure	21.6	34.4	12.8
Violence exposure	32.1	53.3	21.2
Difference (raw)			8.4
Regression: Δ crime $\sim$ any_violence + baseline (weighted)			$p = 0.703$
Regression: Δ crime $\sim$ mean_violence + baseline (weighted)			$p = 0.097$

Notes: Crime rates per 1,000 population at the cuadrante level ($N = 217$). Regressions control for baseline crime and weight by population (2017).

Table A.15: Robustness to Centrality- and Commerce-Specific Time Shocks (Post-normalization)

	Baseline	+CBD×Month	+Commercial×Month	+Both
Violence index × Phase 3	-0.0200^{***}	-0.0152^{**}	-0.0183^{***}	-0.0143^{**}
	(0.0062)	(0.0067)	(0.0059)	(0.0063)
Block FE	Yes	Yes	Yes	Yes
Year-month FE	Yes	No	No	No
municipality×Year FE	Yes	Yes	Yes	Yes
CBD bin×Year-month FE	No	Yes	No	Yes
Commercial density bin×Year-month FE	No	No	Yes	Yes
Observations	467,034	467,034	467,034	467,034
Within R^2	0.27567	0.27565	0.27547	0.27530

Notes: Dependent variable is log price (residential). Standard errors clustered at the block level. Coefficient is per unit of violence intensity in the post-normalization period. * $p < 0.10$, ** $p < 0.05$, *** $p < 0.01$.

Table A.16: Robustness to Centrality- and Commerce-Specific Time Shocks (Post-normalization)

	Baseline	+CBD×Month	+Commercial×Month	+Both
Violence index × Phase 3	-0.0200^{***}	-0.0152^{**}	-0.0183^{***}	-0.0143^{**}
	(0.0062)	(0.0067)	(0.0059)	(0.0063)
Block FE	Yes	Yes	Yes	Yes
Year-month FE	Yes	No	No	No
municipality×Year FE	Yes	Yes	Yes	Yes
CBD bin×Year-month FE	No	Yes	No	Yes
Commercial density bin×Year-month FE	No	No	Yes	Yes
Observations	467,034	467,034	467,034	467,034
Within R^2	0.27567	0.27565	0.27547	0.27530

Notes: Dependent variable is log price (residential). Standard errors clustered at the block level. Coefficient is per unit of violence intensity in the post-normalization period. * $p < 0.10$, ** $p < 0.05$, *** $p < 0.01$.

Table A.17: Pre-trends Joint Test (Event Study Pre-period)

Test	Statistic	Value
Joint Wald test: all pre-period coefficients = 0	F-statistic	1.1545
	p-value	0.2755
	Numerator df	23
	Denominator df	162,612

Notes: Event-study estimated on the pre-period window with block, year-month, and municipality×year fixed effects; standard errors clustered at the block level. The null of no differential pre-trends is not rejected.

Table A.18: Placebo Timing Battery Summary (Pre-shock Only)

Statistic	Value
Number of placebo months	12
Actual post-normal coefficient (baseline)	-0.0200
Placebo coefficient range	$[-0.0051, 0.0108]$
Share of placebos more extreme (two-sided)	0.000

Notes: Each placebo assigns a fake shock month using only pre-2019 data and estimates a two-period pre/post specification. The placebo distribution does not generate effects comparable in magnitude to the true post-normal estimate.

Table A.19: Donut Tests Around Plaza Italia (Post-normalization)

	Excl $<$ 0m	Excl $<$ 250m	Excl $<$ 500m	Excl $<$ 750m	Excl $<$ 1000m
Violence index × Phase 3	-0.0200^{***}	-0.0199^{***}	-0.0197^{***}	-0.0199^{***}	-0.0198^{***}
	(0.0062)	(0.0062)	(0.0062)	(0.0063)	(0.0063)
Block FE	Yes	Yes	Yes	Yes	Yes
Year-month FE	Yes	Yes	Yes	Yes	Yes
municipality×Year FE	Yes	Yes	Yes	Yes	Yes
Observations	467,034	466,939	466,465	465,704	465,061

Notes: Dependent variable is log price (residential). Standard errors clustered at the block level. Excluding transactions close to Plaza Italia leaves the estimate essentially unchanged. * $p < 0.10$, ** $p < 0.05$, *** $p < 0.01$.

Table A.20: Donut Tests Around Alternative Epicenters (Post-normalization)

	Excl < 0m	Excl < 250m	Excl < 500m	Excl < 750m	Excl < 1000m
Plaza Italia					
Violence index × Phase 3	-0.0174^{**}	-0.0173^{**}	-0.0172^{**}	-0.0174^{**}	-0.0175^{**}
	(0.0070)	(0.0070)	(0.0070)	(0.0071)	(0.0072)
Puente Alto					
Violence index × Phase 3	-0.0174^{**}	-0.0173^{**}	-0.0171^{**}	-0.0173^{**}	-0.0172^{**}
	(0.0070)	(0.0070)	(0.0070)	(0.0070)	(0.0071)
Maipú					
Violence index × Phase 3	-0.0174^{**}	-0.0173^{**}	-0.0172^{**}	-0.0168^{**}	-0.0172^{**}
	(0.0070)	(0.0070)	(0.0070)	(0.0070)	(0.0072)
Nearest of the three					
Violence index × Phase 3	-0.0174^{**}	-0.0171^{**}	-0.0168^{**}	-0.0169^{**}	-0.0171^{**}
	(0.0070)	(0.0070)	(0.0071)	(0.0072)	(0.0075)

Notes: This table reproduces donut exclusions around additional epicenters using the specification reported in the corresponding output (period defined with post-normal = `5_post_normal`). All models include block, year-month, and municipality×year fixed effects with standard errors clustered at the block level. * $p < 0.10$, ** $p < 0.05$, *** $p < 0.01$.

Table A.21: Repeat-Sales Robustness (Property Fixed Effects)

	Baseline (Block FE)	Repeat-sales sample (Property FE)
Violence index × Phase 3	-0.0200^{***}	-0.0411^{***}
	(0.0062)	(0.0105)
Block FE	Yes	No
Property FE (Com_rol)	No	Yes
Year-month FE	Yes	Yes
municipality×Year FE	Yes	Yes
Observations	467,034	36,798

Notes: Repeat-sales sample restricts to properties with at least one pre and one post transaction. The property-FE model clusters two-way by property and block (as in the reported output). * $p < 0.10$, ** $p < 0.05$, *** $p < 0.01$.

Table A.22: Spatial Dependence in Inference: Alternative Clustering and Conley SEs

	Block	Block+Month	municipality	Conley 1km	Conley 2km	Conley 5km
Violence index × Phase 3	-0.0200^{***}	-0.0200^{***}	-0.0200^{***}	-0.0200^{***}	-0.0200^{***}	-0.0200^{***}
	(0.0062)	(0.0061)	(0.0048)	(0.0067)	(0.0068)	(0.0035)
Block FE	Yes	Yes	Yes	Yes	Yes	Yes
Year-month FE	Yes	Yes	Yes	Yes	Yes	Yes
municipality×Year FE	Yes	Yes	Yes	Yes	Yes	Yes
Observations	467,034	467,034	467,034	467,034	467,034	467,034

Notes: Dependent variable is log price (residential). All specifications are identical except for the variance-covariance estimator. The Conley 5km specification yields unusually small standard errors in this setting and is not used as the preferred benchmark; 1–2km cutoffs align with clustered inference. * $p < 0.10$, ** $p < 0.05$, *** $p < 0.01$.

Table A.23: Sensitivity to Metro Proximity Threshold in Channel Definitions

Threshold (m)	Main	Violence Only	Metro Only	Both	Triple int.	N_{both}	N_{metro}	N_{viol}	N_{ctrl}
300	−0.0200	−0.0180	−0.0543	−0.0523	−0.0218	5,007	3,574	135,639	322,814
400	−0.0200	−0.0188	0.0093	−0.0318	−0.0183	8,303	6,955	132,343	319,433
500	−0.0200	−0.0174	−0.0060	−0.0343	−0.0133	11,829	11,882	128,817	314,506
600	−0.0200	−0.0181	0.0011	−0.0278	−0.0107	14,883	17,821	125,763	308,567
700	−0.0200	−0.0177	0.0029	−0.0273	−0.0117	18,092	23,756	122,554	302,632
800	−0.0200	−0.0191	−0.0037	−0.0231	−0.0020	21,947	29,603	118,699	296,785

Notes: Reported entries are post-normalization coefficients (per unit violence index) under alternative definitions of being "near" a closed station. "Main" is the baseline post-normal coefficient from the full-sample specification; channel coefficients come from the channel-separation model; "Triple int." is the post-normal interaction term in the triple-difference decomposition. N_{ctrl}, N_{viol}, N_{metro}, N_{both} are transaction counts by channel under each threshold. Standard errors are omitted here for space; Appendix Figure A.12 reports confidence intervals for key channels.

Figures

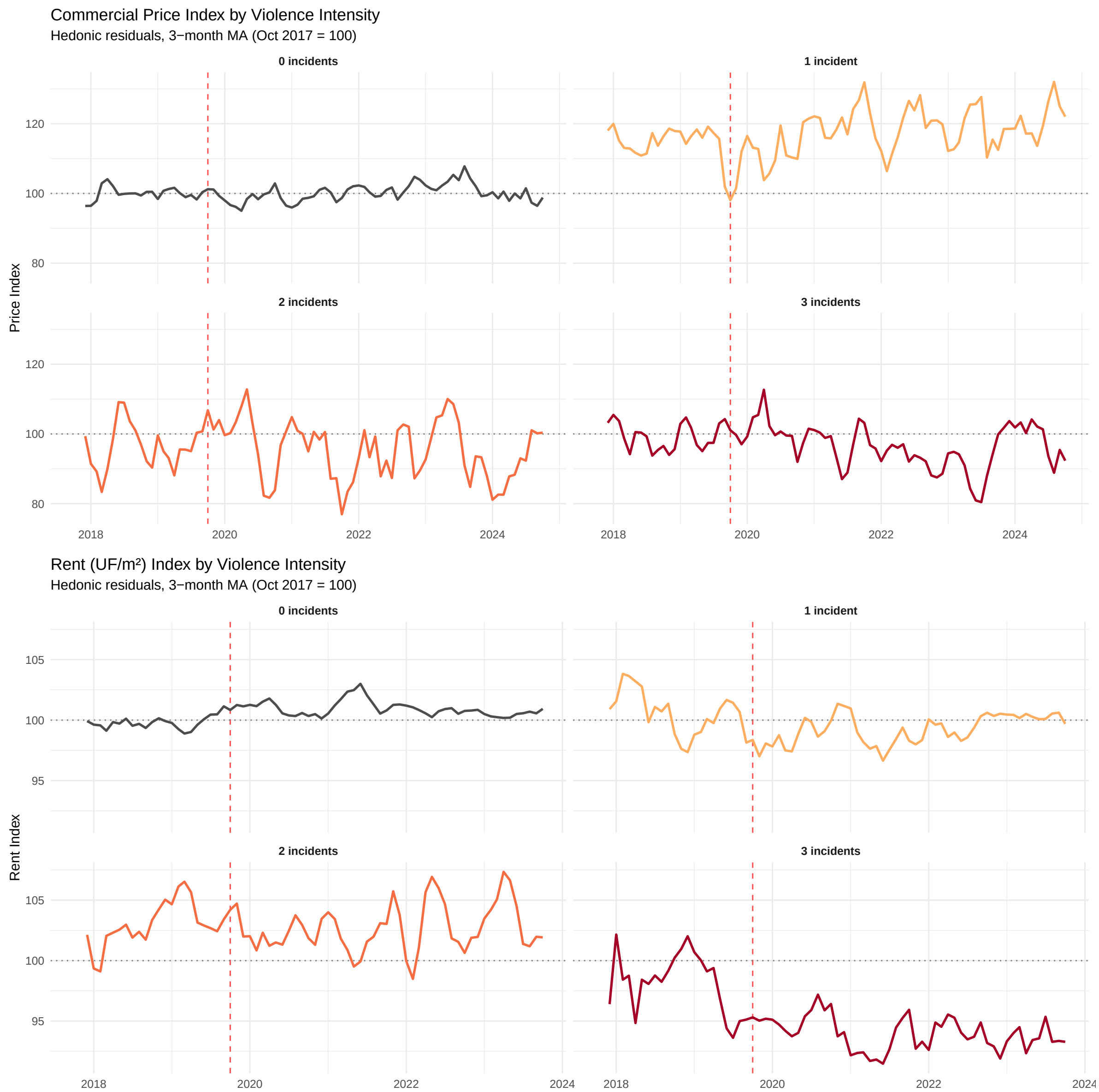

Figure A.1: Commercial and Apartment listing. Hedonic residuals normalized to 100 in October 2017, 3-month moving averages. Vertical dashed line marks October 2019.

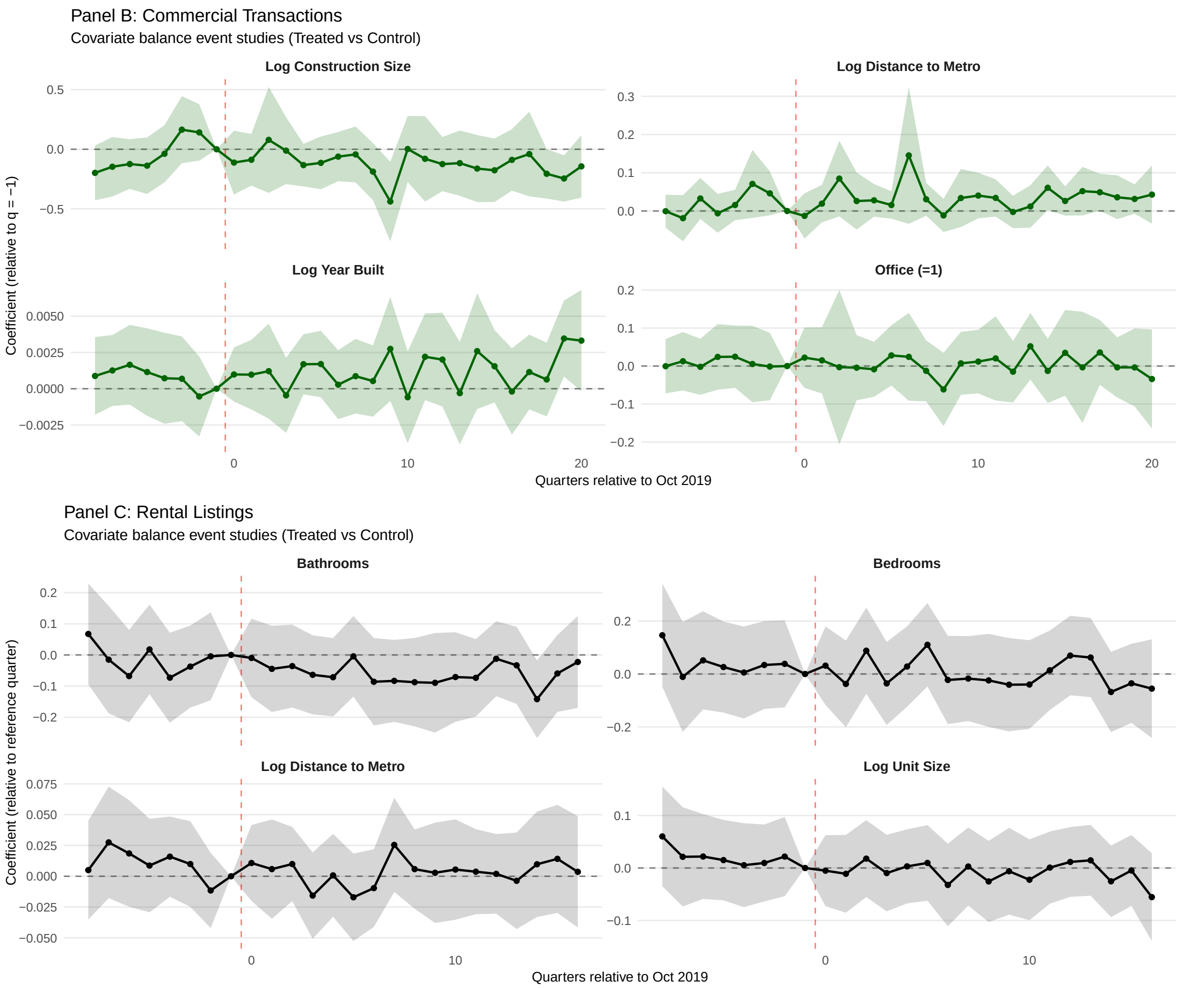

Figure A.2: Covariate Balance Event Studies (Commercial and Apartment listings). Coefficients from regressions of each covariate on treated $\times$ quarter indicators with block and year-month FEs. Bands: 95% CIs, SEs clustered at block level. Reference: Q-1.

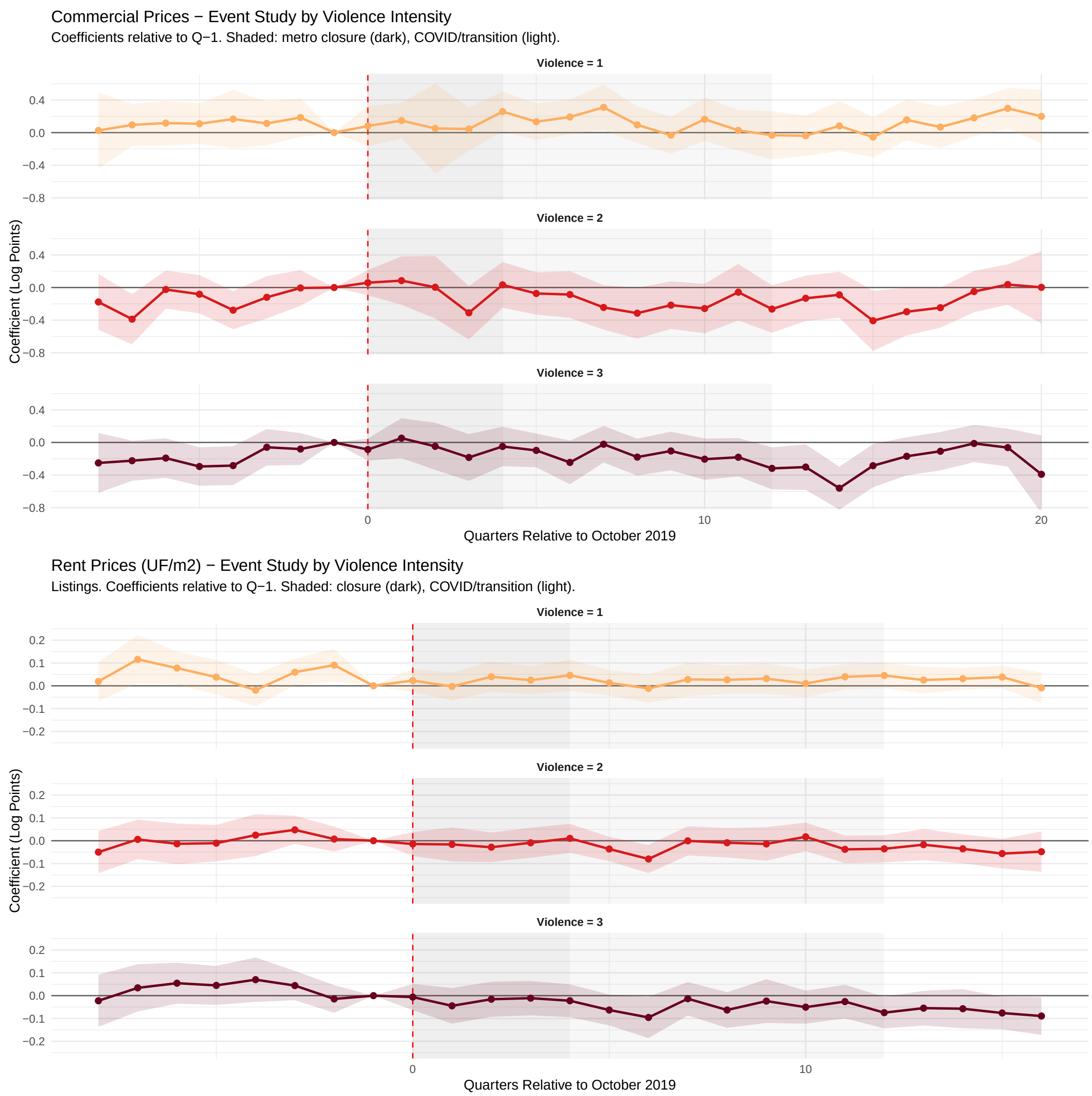

Figure A.3: Commercial Prices and Apartment listings: Event Study by Violence Intensity. Coefficients from a difference-in-differences event-study with interactions between event time (quarters relative to October 2019) and exposure groups ($V = 1, 2, 3$), using $V = 0$ blocks as control. Estimates normalized to $Q{-}1$ (July–September 2019). Model includes block, year-month, and municipality-by-year fixed effects; 95% CIs based on SEs clustered at block level. Shaded regions: Phase 1 (metro closure; darker) and Phase 2 (COVID/transition; lighter); dashed line marks shock onset ($Q0$).

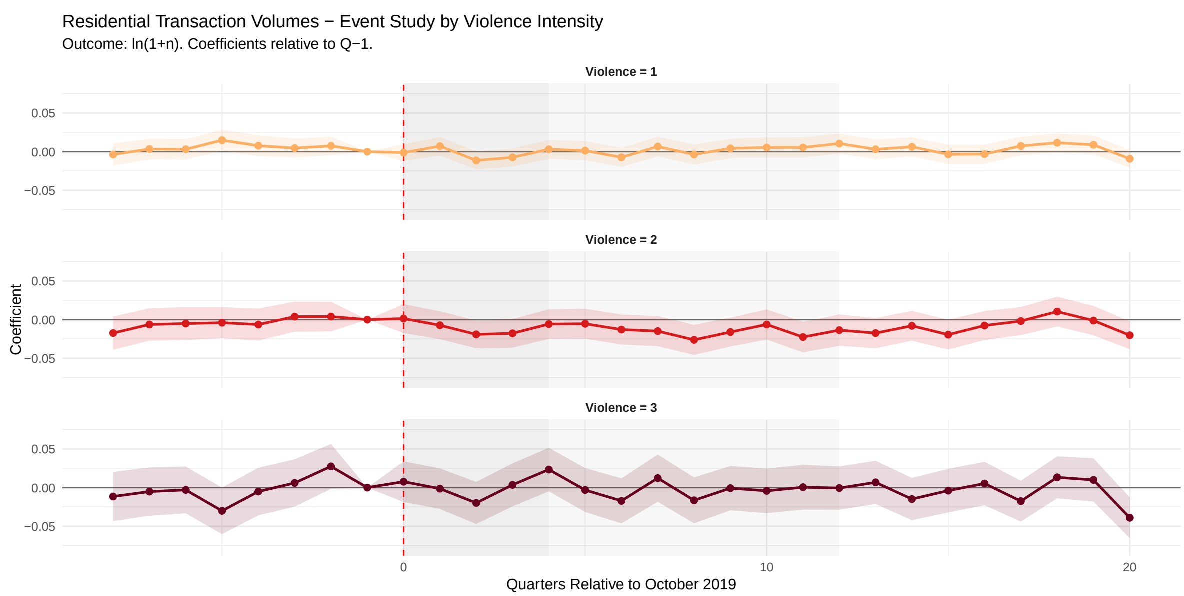

Figure A.4: Residential Transaction Volumes: Event Study by Violence Intensity. Outcome is $\ln(1+n)$ where n is residential transactions per block-quarter. Coefficients by exposure group ($V = 1, 2, 3$) relative to control ($V = 0$), normalized to $Q{-}1$. Model includes block, event-quarter, and municipality-by-year FEs; 95% CIs use SEs clustered at block level.

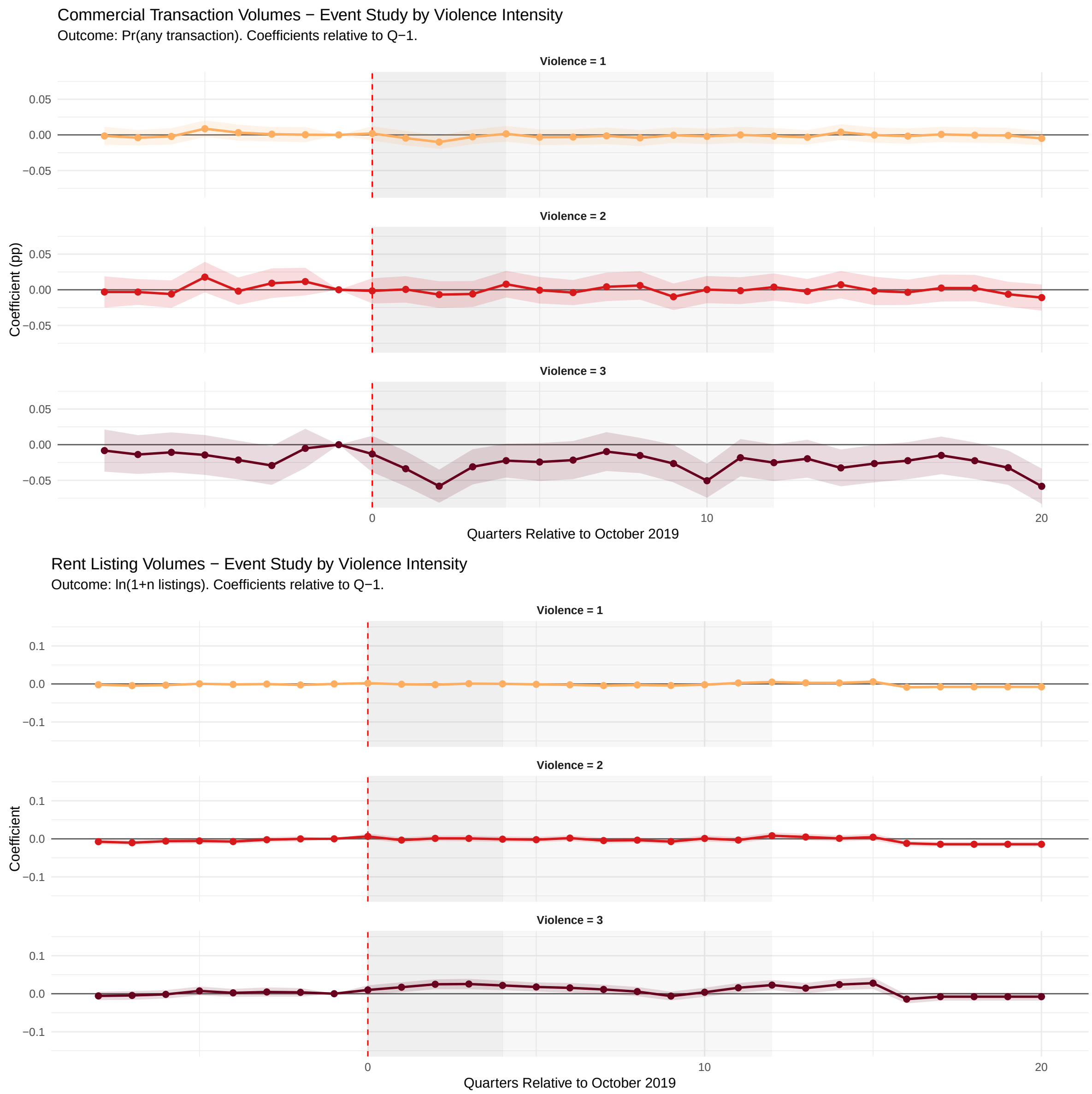

Figure A.5: Residential Transaction Volumes: Event Study by Violence Intensity. Outcome is an indicator for any commercial transaction in a block-quarter (linear probability model), reported in percentage-point units. Coefficients are event-study estimates by exposure group ($V = 1, 2, 3$) relative to control blocks ($V = 0$), normalized to $Q{-}1$ (July–September 2019). The model includes block (manzana) fixed effects, event-quarter fixed effects, and municipality-by-year fixed effects; 95% confidence intervals use standard errors clustered at the block level (manzana). Shaded regions denote metro closure (darker) and COVID/transition (lighter), and the dashed line marks $Q0$ (October 2019)..

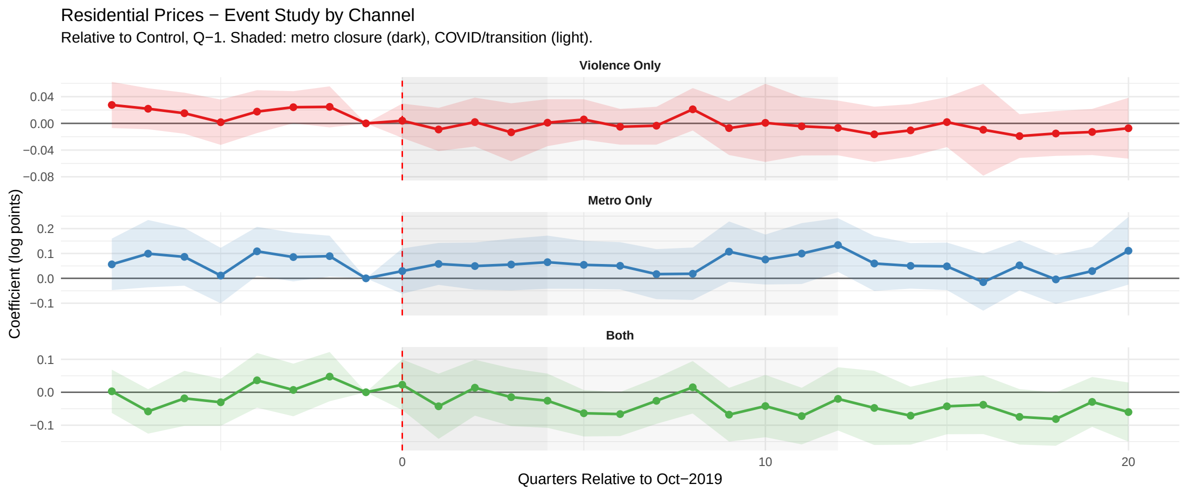

Figure A.6: Residential: Event Study by Treatment Channel

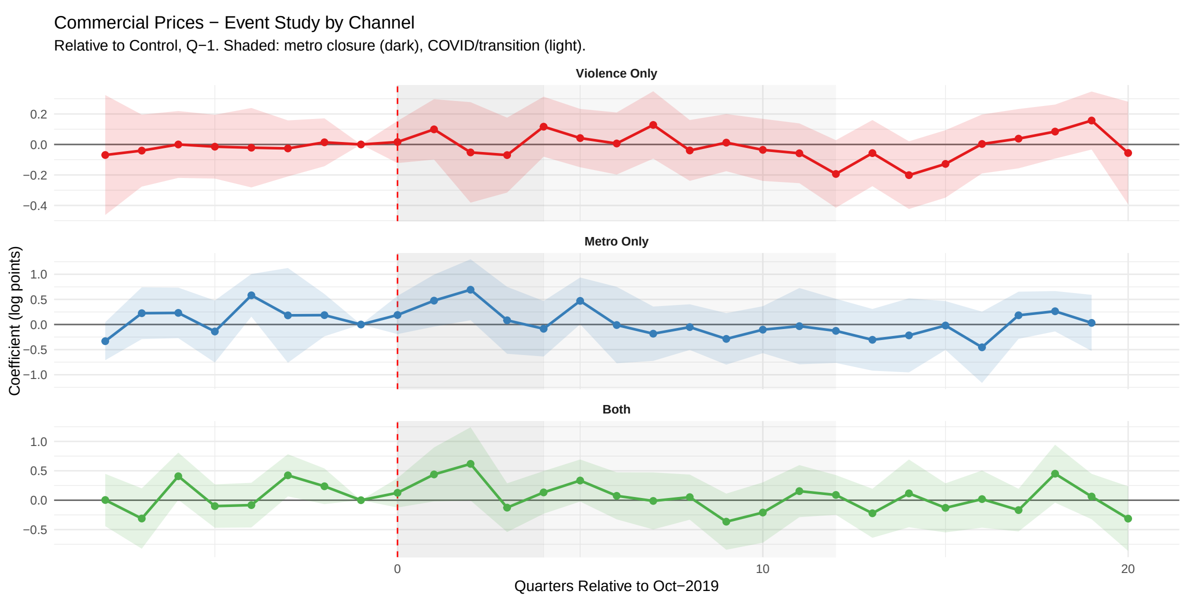

Figure A.7: Commercial: Event Study by Treatment Channel

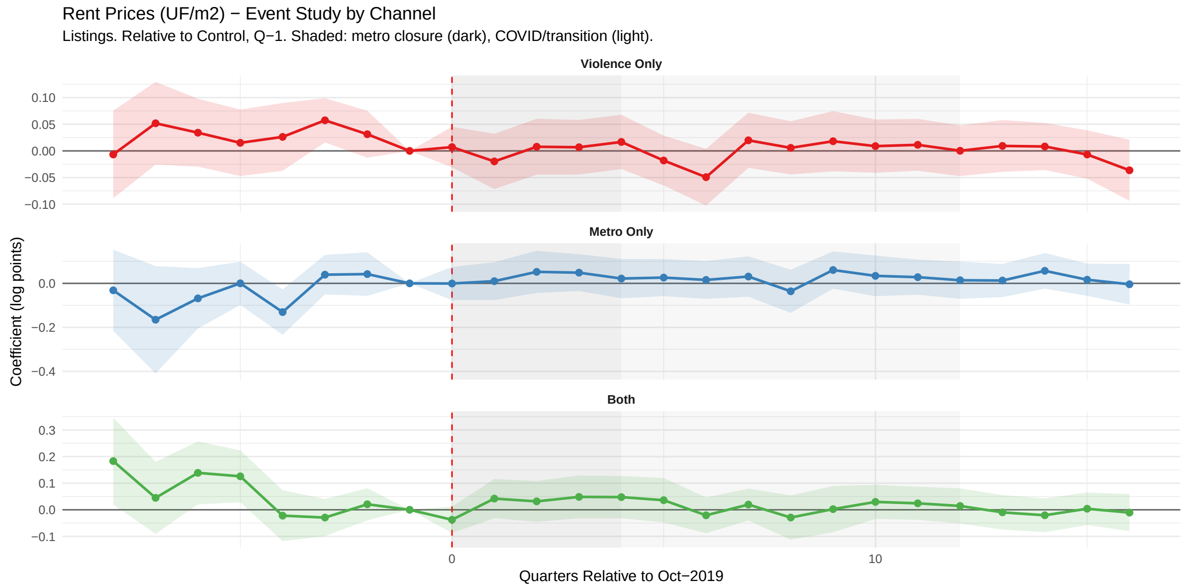

Figure A.8: Listings: Event Study by Treatment Channel

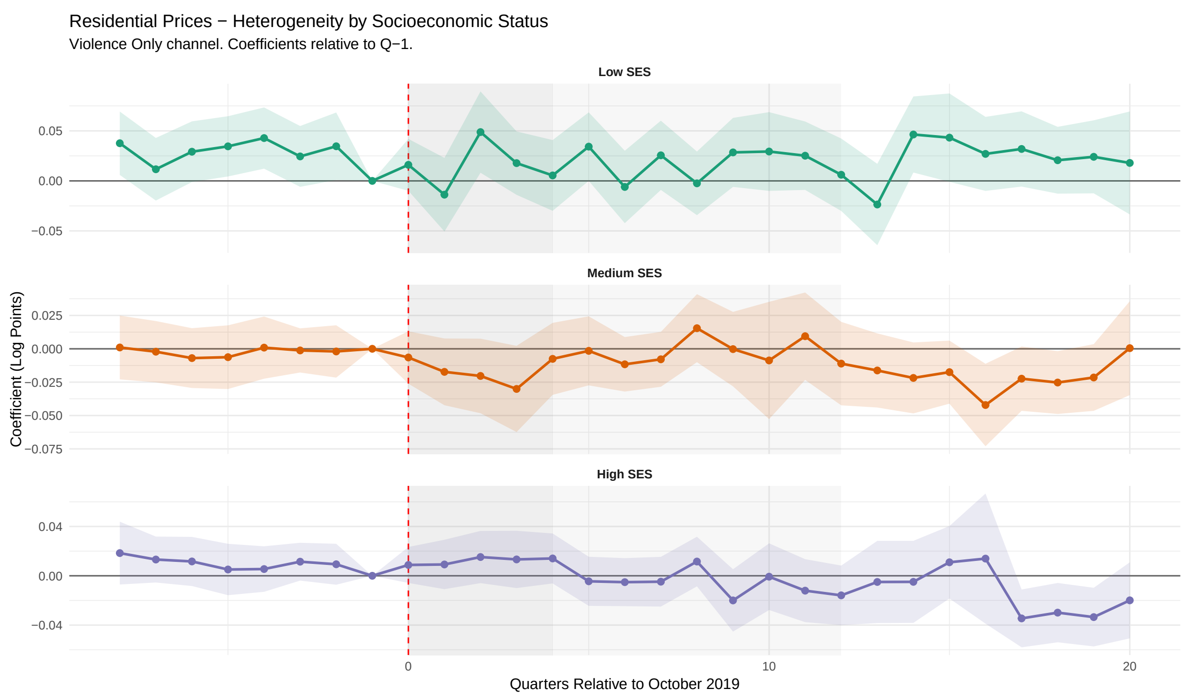

Figure A.9: Residential: Event Study by Socioeconomic Status (GSE)

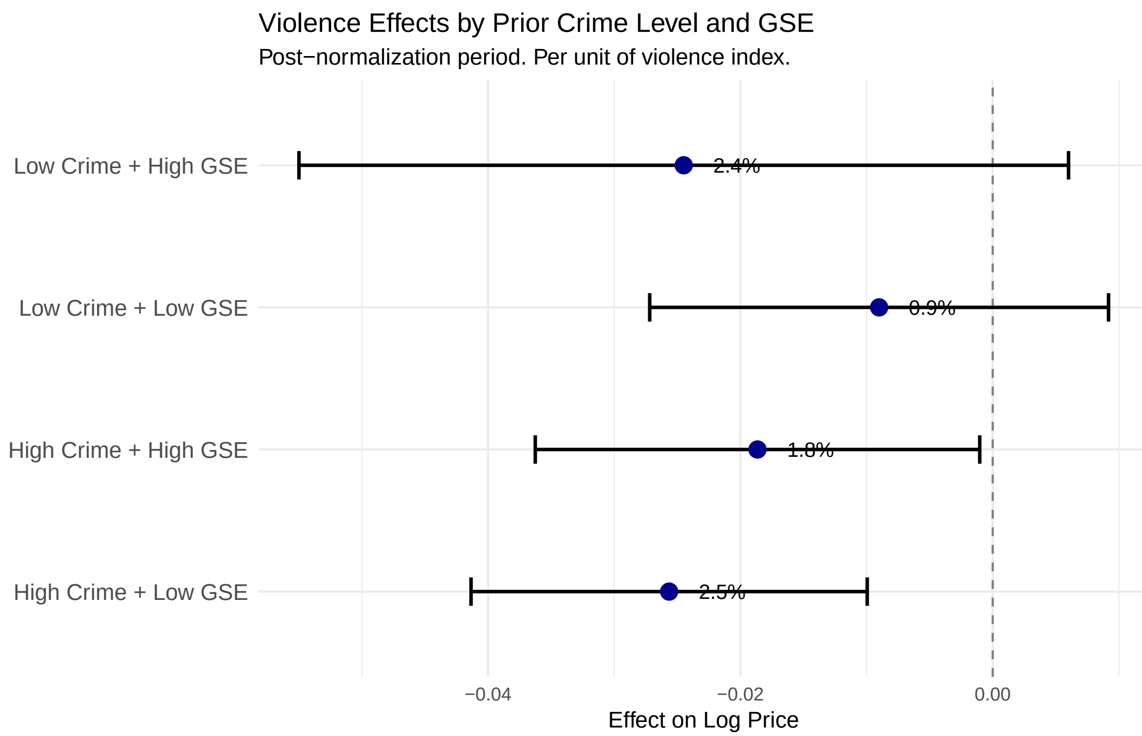

Figure A.10: Residential: Violence Effects by Prior Crime and GSE

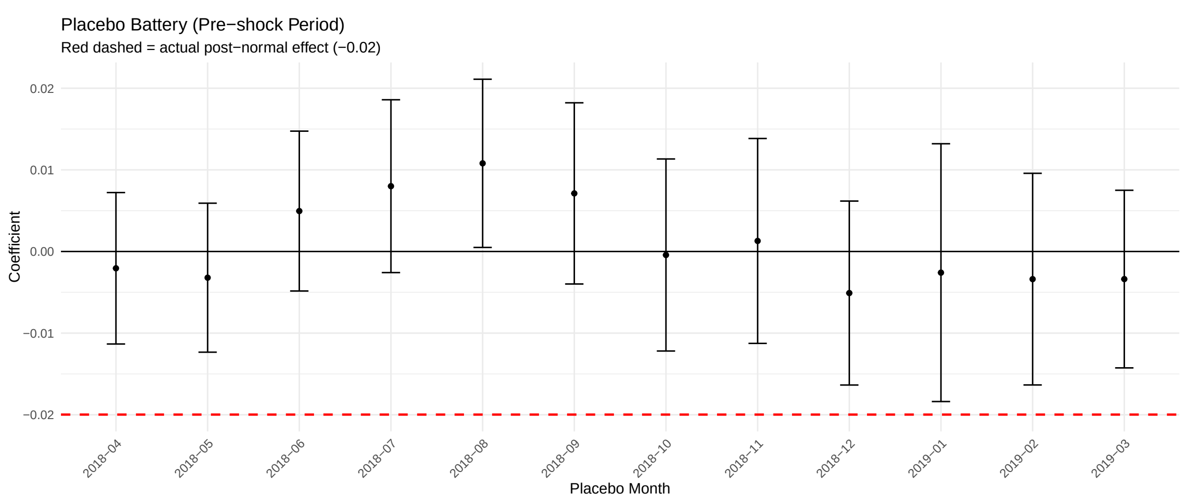

Figure A.11: Residential: Event Study by Socioeconomic Status (GSE)

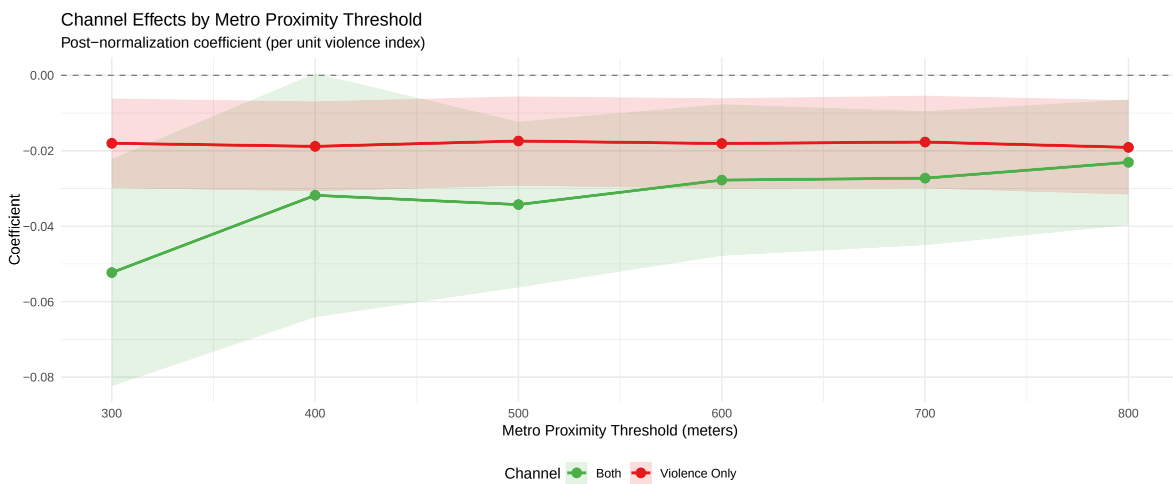

Figure A.12: Residential: Violence Effects by Prior Crime and GSE